Assessing the impacts of shoreline hardening on beach response to hurricanes: Saint-Barthélemy, Lesser Antilles

Valentin Pillet, Virginie K.E. Duvat, Yann Krien, Raphaël Cécé, Gael Arnaud, Cécilia Pignon-Mussaud

Assessing the impacts of shoreline hardening on beach response to hurricanes: Saint-Barthélemy, Lesser Antilles

Accepted manuscript

Pillet, V., Duvat, V.K.E., Krien, Y., Cécé, R., Arnaud, G., Pignon-Mussaud, C., 2019. Assessing the impacts of shoreline hardening on beach response to hurricanes: Saint-Barthélemy, Lesser Antilles. Ocean Coast. Manag. 174, 71–91. https://doi.org/10.1016/j.ocecoaman.2019.03.021

Authors

Valentin Pillet, PhD candidate

UMR LIENSs 7266, University of la Rochelle-CNRS, 2 rue Olympe de Gouges, 17000 La Rochelle – France

valentin.pillet@univ-lr.fr

Virginie K.E. Duvat, Pr

UMR LIENSs 7266, University of la Rochelle-CNRS, 2 rue Olympe de Gouges, 17000 La Rochelle – France

virginie.duvat@univ-lr.fr

Yann Krien, Dr

University of the West Indies, UFR Sciences, Campus de Fouillole, 97159 Pointe-à-Pitre, Guadeloupe – France

ykrien@gmail.com

Raphaël Cécé, Dr

University of the West Indies, UFR Sciences, Campus de Fouillole, 97159 Pointe-à-Pitre, Guadeloupe – France

raphael.cece@univ-antilles.fr

Gael Arnaud, Dr

University of the West Indies, UFR Sciences, Campus de Fouillole, 97159 Pointe-à-Pitre, Guadeloupe – France

gael.arnaud@univ-antilles.fr

Cécilia Pignon-Mussaud, Eng

UMR LIENSs 7266, University of la Rochelle-CNRS, 2 rue Olympe de Gouges, 17000 La Rochelle – France

cecilia.pignon-mussaud@univ-lr.fr

First Author: Valentin Pillet, PhD candidate

UMR LIENSs 7266, University of la Rochelle-CNRS
2 rue Olympe de Gouges, 17000 La Rochelle, France
+33516497623, valentin.pillet@univ-lr.fr

ORCID : 0000-0002-2787-2648

Assessing the impacts of shoreline hardening on beach response to hurricanes: Saint-Barthélemy, Lesser Antilles

1. Introduction

It is widely acknowledged that the physical characteristics of small tropical islands (i.e. small size and concentration of human assets in low-lying coastal areas) make them among the most vulnerable territories to the impacts of low-frequency high-intensity events, such as tropical cyclones (Pelling and Uitto, 2001; Duvat, 2008; Hay and Mimura, 2010; Giuliani et al., 2011; Nurse et al., 2014; Duvat et al., 2016; Duvat et al., 2017a).

Tropical cyclones (TCs) have been the subject of numerous studies, and their impacts on coastal morphology, marine and terrestrial ecosystems and human societies are well known (Bush, 1991; Scoffin, 1993; Cahoon et al., 2003; Cazes-Duvat, 2005; Scheffers and Scheffers, 2006; Morton et al., 2008; Mallela and Crabbe, 2009; Scopélitis et al., 2009; Angelucci and Conforti, 2010; Caron, 2011; Etienne, 2012; Strobl, 2012; Duvat et al., 2016). TCs' impacts on small tropical islands' coasts are generally severe, and they can be either erosive, or accretional (Baines et al., 1974; Bayliss-Smith, 1988; Scoffin, 1993; Ford and Kench, 2014, 2016; Duvat et al., 2016; Duvat et al., 2017b). In the supratidal area, beach sediment loss resulting from cyclonic waves action can cause a decrease in beach thickness (Duvat et al., 2016) and a retreat of the upper beach, with cliff cutting in sand dunes, as observed on Rodrigues Island (Indian Ocean) after TC Kalunde in March 2003 (Cazes-Duvat, 2005). However, TCs may also be constructional, i.e. inject fresh material into the sedimentary system, by transferring large volumes of sediment to the coast that may cause a marked development of beaches (Bush, 1991; Ford and Kench, 2014; Duvat et al., 2016, 2017b). Importantly, some studies reported storm-generated features composed of sand or of coral debris (Scoffin, 1993; Morton et al., 2008; Caron, 2011), as illustrated by the remarkable storm rampart generated by TC Bebe in October 1972 on Funafuti, Tuvalu (Maragos et al., 1973; Baines et al., 1974; Baines and McLean, 1976). Furthermore, cyclonic waves can transfer sediments to inner land areas over great distances (Duvat and Pillet, 2017; Rey et al., 2017). For example, overwash processes led to the deposition of sand, coral debris and blocks over distances that reached up to 70 m from the pre-cyclone vegetation line on Tubuai and Reunion islands, respectively in 2010 (TC Oli; Etienne, 2012) and 2014 (TC Bejisa; Duvat et al., 2016). In natural settings, sand and coral debris deposited by TCs may thus contribute to an increase in the elevation of low-lying coastal areas (Duvat et al., 2017b; Duvat et al., 2019). In contrast, in highly-developed settings, these deposits are often quickly removed and used for construction (Bush, 1991), which annihilates the abovementioned positive effect of TCs. Importantly, several studies emphasized the high spatial variability of cyclone-induced

morphological changes on small islands' coasts over short distances, and even on the sediment cell scale (Cazes-Duvat, 2005; Etienne, 2012; Duvat et al., 2016; Duvat et al., 2019). The nature (erosional vs. accretional) and severity of TC impacts are function of a variety of factors, including the cyclone track, island and shoreline exposure (which decreases with the presence of nearshore islets and of protruding headlands), the coastal system's geomorphic characteristics (i.e. type, dimensions, elevation, sediment composition, presence or absence of coral reef, etc.), the extent, nature and density of the coastal vegetation, and the degree of anthropogenic disturbance, especially the extent of longitudinal defence structures (Stoddart, 1963, 1965; Bush, 1991; Scoffin, 1993; Cambers, 2009; Duvat et al., 2016; Duvat et al., 2017b).

On those islands exhibiting limited low-lying exploitable land, rapid population growth and economic development (including tourism-related), urbanization and development generally led to the concentration of inhabitants, buildings and infrastructures in low-lying coastal areas, which are highly exposed to sea-related hazards (Rivera-Monroy et al., 2004; Nurse et al., 2014). This has in turn often led to the construction of coastal defence structures along the shoreline (Romine and Fletcher, 2012; Duvat, 2013; Duvat et al., 2016). Some case studies showed that human disturbances can be a major forcing factor of coastal and shoreline change, e.g. driving high rates of shoreline retreat during cyclonic events (Duvat et al., 2016). Cooper and Pile (2014) especially highlighted the damaging effect of seawalls on beaches fronting them. Once built, these structures no longer allow the beach to retreat inland under extreme wave events. Instead, the reflection of storm waves by these structures contributes to beach narrowing by increasing erosion (Bush, 1991; Fletcher et al., 1997), which eventually leads to beach loss (Schlacher et al., 2006; Cambers, 2009; Cooper and Pile, 2014). Additionally, the establishment of tourist amenities in coastal areas has led, in many cases, to the destruction and replacement of the native vegetation by introduced species, which decreases the resistance and the resilience of coastal systems to TC impacts (Cambers, 2009; Duvat et al., 2016; Duvat et al., 2017b; Duvat et al., 2019).

Multi-date aerial image analysis using GIS techniques are widely employed to assess TC impacts, including change in shoreline position. Although the seaward edge of the vegetation is the most common shoreline proxy used to assess the impacts of TCs (e.g. Ford and Kench, 2014, 2016), some studies employed either other, or additional shoreline proxies, including the base of the beach and the landward limit of cyclonic deposits, to better capture the wide range of changes caused by TCs to sedimentary systems (Duvat and Pillet, 2017; Duvat et al., 2017b, c). However, with the exception of a limited number of studies (e.g. Duvat et al., 2016; Salmon et al., 2019), the role of anthropogenic factors in driving TCs' morphological impacts on small tropical islands was paid little attention to date. In fact, previous studies mostly emphasized the multi-decadal impacts of human activities on shoreline

change, including the impacts of aggregate mining, dredging in reef flats and the construction of coastal defence structures (Bush, 1991; Cambers, 2009; Biribo and Woodroffe, 2013; Mann and Westphal, 2014; McLean and Kench, 2015; Aslam and Kench, 2017). Yet, because they modify both coastal systems and hydrodynamic processes, anthropogenic activities should be more systematically considered when assessing TCs' impacts on coastal systems. Better understanding how they modify the response of coastal systems to TCs' impacts, and thereby influence the trajectory of vulnerability of these systems over time, is critical for the design of appropriate (i.e. context-specific) risk management policies (i.e. improvement of human security and reduction of damage) in already-developed coastal areas and of well-adapted development strategies in newly-built coastal areas.

This article contributes filling this research gap by investigating the contribution of anthropogenic disturbances to the variability of the impacts of Category 4 to 5 hurricanes Irma, Maria and José, on the coastal systems of the Caribbean island of Saint-Barthélemy. Based on multi-date satellite imagery analysis and on a post-hurricane field survey, it more specifically addresses three questions: (1) What were the impacts of these hurricanes on shoreline position and on coastal morphology? (2) To what extent did anthropogenic disturbances drive the diversity and the spatial variability of these hurricanes' impacts on shoreline position and on beach response? (3) More generally, how to attribute observed hurricane impacts to specific anthropogenic drivers? To address this key question, this paper proposes a new methodological protocol based on the inclusion of human disturbances in shoreline change analysis.

First, we will present the methodology used, based on geomatics and fieldwork. Second, the high spatial variability of the impacts of September 2017 hurricanes on shoreline position and coastal morphology will be presented. Third, we will discuss the drivers of the variability of these hurricanes' impacts, especially the role of anthropogenic disturbances, and the interest of using geomatics to quantify the contribution of the latter. The implications of findings for disaster risk reduction and future coastal development will finally be discussed.

2. Context of the study

2.1 Saint-Barthélemy Island

2.1.1. Main physical features

Saint-Barthélemy Island, which is a French overseas territory, is located in the northern part of the Lesser Antilles Arc and lies at 17°53N and 62°49W (Fig. 1). It is a small V-shaped island, extending about 16 km (from west to east) by 3 km (from north to south), with a total land area of 21 km² (Fig. 2). Saint-Barthélemy is a mountainous island with a highly irregular topography (the highest point is Morne de Vitet, 286 m). Its landscape is characterized by the succession of numerous valleys coming out on coastal plains on their oceanward extremities. Its coastline is composed of rocky shores alternating with sandy beaches generally occurring in embayments (Caron, 2011; Fielding, 2017). Saint-Barthélemy exhibits two beach types: (1) beaches backing onto coastal plains or rocky slopes, and (2) barrier beaches bordered by a lagoon where mangroves can be found locally. The former type is the most common and is found all around the island. The latter type is less represented and can be found at five sites (Fig. 2), where alluvium and sand have filled low-lying areas (Christman, 1953). Barrier beaches are low, rarely exceeding 4 m in elevation (i.e. ranging from 1 m at Petit Cul-de-Sac to 4 m at Grande Saline), and narrow with widths ranging from 60 m (Grand Cul-de-Sac) to 300 m (Grande Saline). Beaches are mainly composed of coral sand (Table 1). In the southeast (i.e. Toiny and Grand Fond), due to the presence of fringing coral reefs and to increased exposure to hurricanes, beaches are composed of cobble-sized coral debris (Caron, 2011) (Table 1).

In this region, the climate is tropical. Trade winds generate waves from the east-northeast to southeast that do not exceed 3 m in height in the open ocean. However, tropical depressions and hurricanes are frequent in the Caribbean between June and November (10 hurricanes in 2017 in this region), with high-energy wave events that can easily reach and even exceed 3 m at the coast. Additionally, between November and March, large groundswells generated by slow moving distant low-pressure systems can reach this region (Cooper et al., 2013). The mean tidal range is around 0.5 m (Caron, 2011).

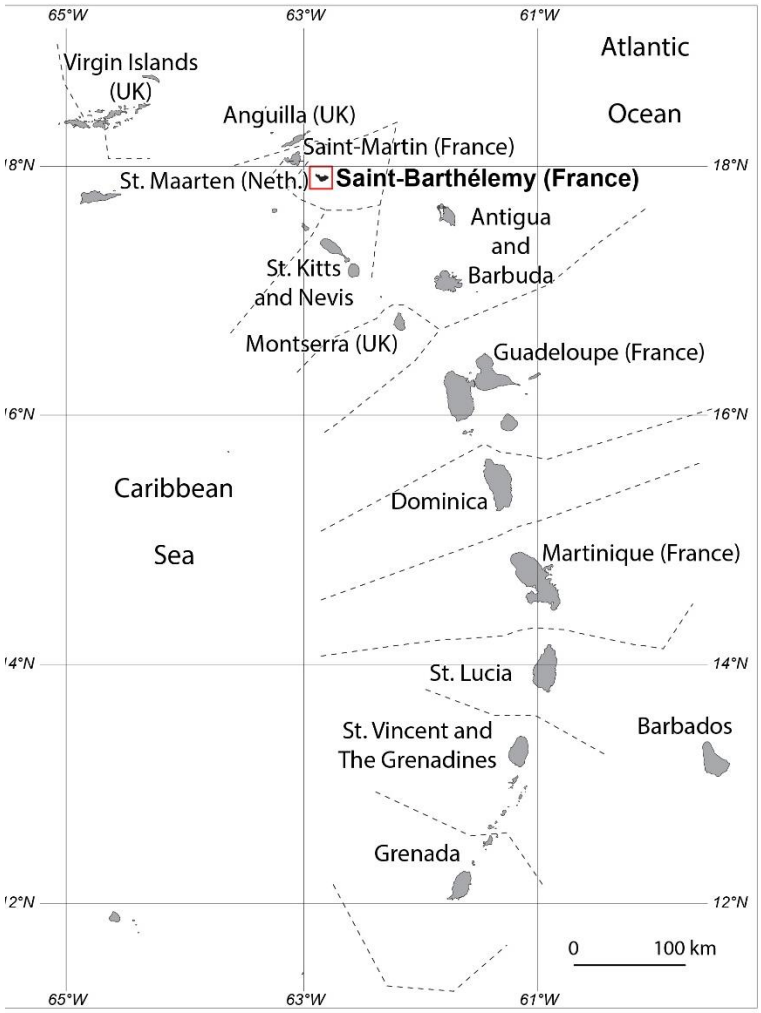

Fig. 1. Location map of Saint-Barthélemy Island in the Lesser Antilles region.

Beach number and name	Physical features					Anthropogenic features				
	Reef type	Presence of nearshore islet	Sediment type	Presence of beachrock slabs[1]	Beach vegetation type	Coastal urbanisation	Presence of tracks or breaches through the sedimentary system	Vegetation clearing (C) or removal (R)	Shoreline armouring or seaside property walls	Transversal engineered structures
1. Anse de Colombier	/	No	Coral sand	Yes	/	No	No	No	No	No
2. Anse des Flamands	/	Yes	Coral sand	Yes	Mixed	Yes	Yes	Yes (R)	Yes	No
3. Anse des Cayes	Fringing	No	Coral sand	Yes	No data	Yes	Yes	Yes (R)	Yes	No
4. Baie de Saint-Jean	Fringing	No	Coral sand	No	Mixed	Yes	Yes	Yes (R)	Yes	No
5. Anse de Lorient	Fringing	No	Coral sand	Yes	Mixed	Yes	Yes	Yes (R)	Yes	No
6. Anse de Marigot	Fringing	Yes	Coral sand	Yes	Introduced	No	Yes	Yes (R)	No	No
7. Anse du Grand Cul-de-Sac	Fringing	Yes	Coral sand	Yes	Introduced	Yes	Yes	Yes (R)	Yes	No
8. Anse du Petit Cul-de-Sac	Fringing	No	Coral sand	Yes	Mixed	No	Yes	No	No	No
9. Anse Toiny	Fringing	No	Coral sand and debris	Yes	Indigenous	No	Yes	Yes (R)	No	No
10. Anse de Grand Fond	Fringing	No	Coral sand and debris	Yes	Indigenous	No	Yes	No	No	No
11. Anse de Grande Saline	No	Yes	Coral sand	Yes	Indigenous	No	Yes	Yes (C)	No	No
12. Anse du Gouverneur	No	No	Coral sand	Yes	Indigenous	No	Yes	Yes (C)	No	No

Table 1. Main characteristics of Saint-Barthélemy Island beaches.

[1] Based on Caron (2012) and on field observations (2005-2007 and 2017)

2.1.2. Main human features

In 2014, Saint-Barthélemy had a total population of 9,427 inhabitants (INSEE, 2013), i.e. 373 inhab./km^2. The population has been steadily growing since the 1970s. Residents mainly concentrate first, in the main city of Gustavia in the south, which provides one of the best natural harbours in the region (Fielding, 2017), and second, on the northern leeward coast (Flamands, Cayes, Saint-Jean, Lorient, Grand Cul-de-Sac). Most of the southern bays are sparsely populated or uninhabited (Fig. 2). In Saint-Barthélemy, tourism represents the first economic activity and, in 2006, it was the first employment sector of the island (37% of total paid jobs, INSEE, 2009). Since the 1970s, the development of tourism has benefited from real estate market, with the number of visitors gradually increasing to reach a peak in 1997 (370,000 tourists). Since then, the number of visitors reached around 300,000 visitors per year (IEDOM, 2018).

Constant population growth associated with the development of the tourism sector has led to increasing pressure on land. As on numerous small mountainous tropical islands, the morphological configuration of the island constrained inhabitants to settle in highly-exposed low-lying coastal areas. The high exposure of buildings to sea-related hazards has progressively led to the construction of longitudinal coastal defence structures aimed at fixing the shoreline and protecting human assets (i.e. buildings, properties, roads) (Fig. 2). On Saint-Barthélemy, these structures are generally composed of uniform-size rocks (i.e. riprap) or of cemented vertical seawalls. In addition, urbanization and beach tourism development have led to the modification, i.e. clearing, entire removal or replacement, depending on coastal sites, of the indigenous vegetation (Table 1).

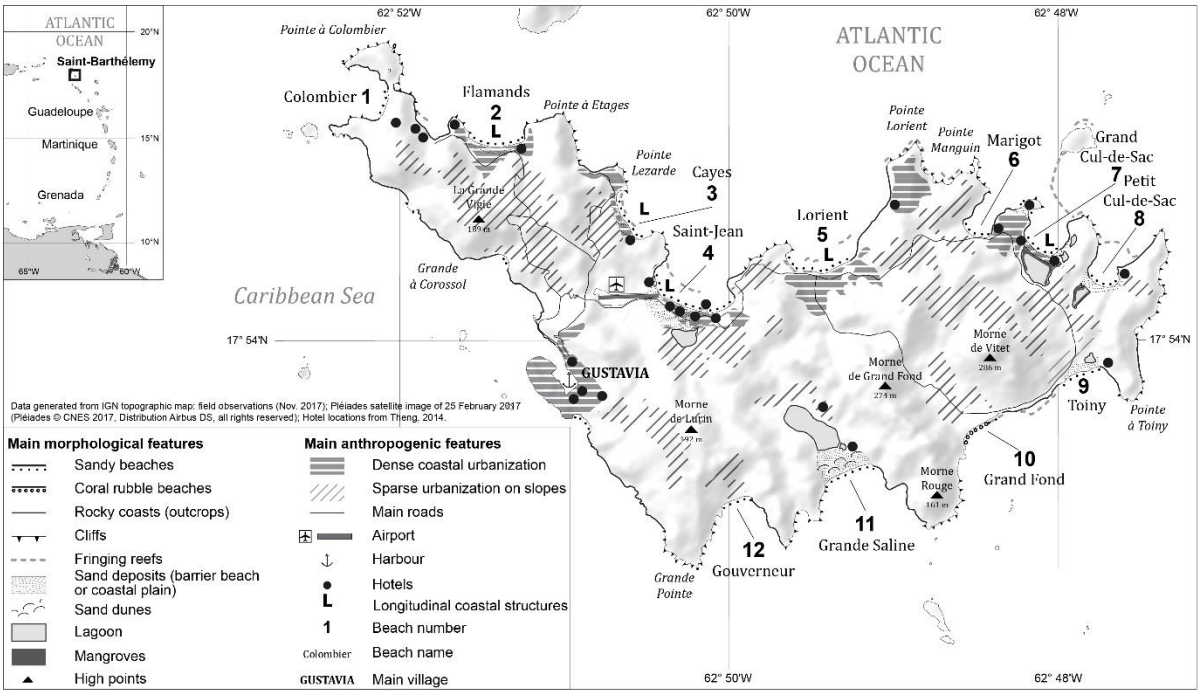

Fig. 2. Main geomorphic and human characteristics of Saint-Barthélemy Island**.**

2.2 Hurricanes Irma, José and Maria (September 2017)

2.2.1 Hurricane season 2017

The 2017 Atlantic hurricane season, which began in May with hurricane Arlene, was particularly active because of meteorological settings that led to a convective environment (i.e. weak El Niño, increase of the tropical Atlantic Ocean temperature from late May, trade winds weakening induced by the temperature rise). In less than two weeks, two category 5 hurricanes occurring simultaneously and 3 major events hit the Leeward Islands. Two of them, Irma and José (Fig. 3a), struck Saint-Barthélemy and Saint-Martin.

2.2.2. Hurricane Irma

On August 30th, a tropical depression located at 370 km west off Cape Verde was upgraded to a tropical storm named Irma by the National Hurricane Centre (NHC). On August 31st, Irma upgraded to a category 1 hurricane, while still in the eastern Atlantic, 740 km off Cape Verde. Irma reached the category 3 in two days (09/01/2017). On September 4th, after shifting direction (south southwest), the hurricane reached up category 4 because of warmer water, while it was approaching the Lesser Antilles. According to Cangialosi et al. (2018), Irma's maximum intensity (288 km/h) was reached from September 5th at 18:00 UTC to September 6th 20:00 UTC. Landfall on Saint-Barthélemy occurred during its maximum intensity, on September 6th around 10:00 UTC

(Degrace, 2017). Irma was the first category 5 hurricane of the season to make landfall on Saint-Barthélemy. Of note, 1 min-sustained winds were up to 288 km/h, with a minimum pressure of 915.9 mb. An unofficial observation in Saint-Barthélemy reported a maximum wind gust of 320 km/h (Cangialosi et al., 2018).

2.2.3. Hurricane José

As Irma, José was a Cape Verde hurricane, formed from a tropical disturbance on August 31st. The tropical storm named José was upgraded to a category 1 hurricane on September 6th at 18:00 UTC, while travelling westward across the Atlantic Ocean (approximately 1,850 km east of the Lesser Antilles Arc). In 24 hours, a rapid intensification brought José to category 3. Its maximum winds velocity peaked at 250 km/h from 18:00 UTC on September 8th to 00:00 UTC on September 9th (Berg, 2018). The minimum estimated central pressure was 938 mb (8th September). On September 9th hurricane José was recorded at 85 km from the northeast of Barbuda. Nevertheless, because of its close approach, the hurricane may have produced sustained tropical-storm-force winds on Saint-Barthélemy. However, no wind observations were available from those islands during José, since wind instruments were damaged or destroyed during hurricane Irma (Berg, 2018).

2.2.4 Hurricane Maria

Maria was the last hurricane of the series. It originated on September 16th from a tropical depression (located at 12°3'N and 52°6'W) that moved westward and then west-north-westward towards Martinique Island. Maria rapidly intensified into a major hurricane and reached the category 5 just before landing on Dominica. According to its path, Maria had limited consequences on Saint-Barthélemy (passing 150 km from the island). However, the wind gusts exceeded 300 km/h and the minimum pressure was about 920 hPa.

2.2.5. Numerical simulations

Atmospheric simulations were performed using the WRF-ARW model (Skamarock et al., 2008) and a high-resolution domain of 0.4 km. This sub-kilometer scale allowed to obtain a preliminary coarse overview of gusts distribution over a 5 km-wide island like Saint-Barthélemy. In order to better take into account the complex shorelines of Saint-Barthélemy and improve the simulation of induced wind effects, a forthcoming study will include micro-scale resolution of 100 m (Cécé et al., 2014, 2016). The 6 hourly ECMWF operational analyses with 0.1° resolution were used as initial and boundary conditions. The results (Fig. 3b) show maximum surface winds on the north coast of Saint-Barthélemy (Anse Colombier), with gusts of 305 km/h. The second coastal area with large gusts is the northeast side from Saint-Jean to Anse du Petit Cul-de-Sac, with wind speeds above

260 km/h. The south coast, in the lee of the stream flow, was relatively sheltered from strong winds (maximum wind speeds reach 230 km/h). The Gustavia Marina would be the less affected area (wind gust of 165 km/h).

A wave-current coupled model (Zhang et al., 2016) was also used to compute maximum significant wave heights for both Irma and José (Fig. 3c). The computational domain extends from 67.5°W to 46°W, and 13.5°N to 27°N, with resolutions spanning from 5 km in the deep ocean to 100 m near the coasts. The model is forced by tides (12 harmonics constituents) as well as wind and pressure fields computed by blending CFSR data with the Holland (1980) and Emanuel and Rotunno (2011) parametric models. Further details on the wind model (denoted E11H80) and its expected performance can be found in Krien et al (2018). The bathymetric data were extracted from navigational charts established by the SHOM. The results suggest that the east coast was the most impacted by the waves during Irma, with significant wave heights that could have reached, and possibly exceeded, 10 m. Conversely, the west coast was less exposed, with 2-3 m waves coming from the north-west or west during the peak of the event. In comparison, the waves were much less energetic for José, with significant wave heights lower than 4-5 m and 1 m for the east and west coasts, respectively.

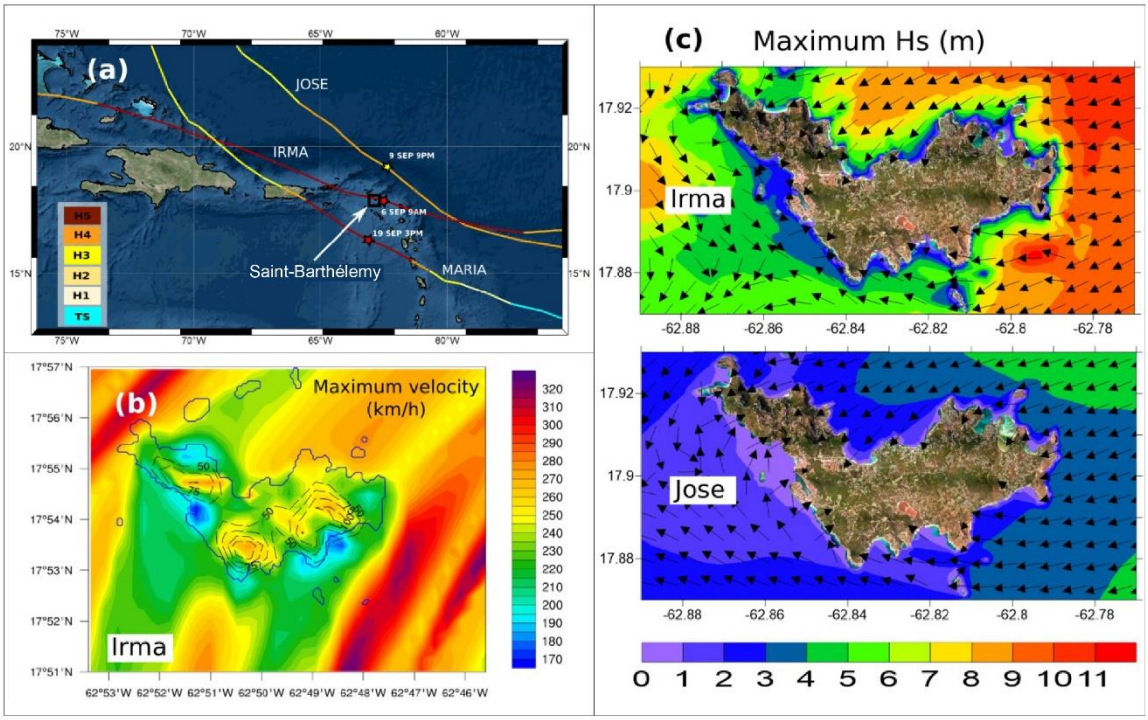

Fig. 3. Main characteristics of September 2017 hurricanes in the Lesser Antilles area. (a) track and intensities of Irma, José and Maria, given by the NHC advisories. The black rectangle indicates the study area. Times are given in UTC. (b) maximum surface winds for Irma at Saint-Barthélemy, computed using the atmospheric model WRF-

ARW at 0.4 km resolution. (c) maximum significant wave heights (in meters) and corresponding mean wave directions (vectors) for Irma and José.

3. Materials and methods

3.1. Hurricane-induced shoreline change assessment

3.1.1. Acquisition and preparation of pre- and post-hurricane satellite imagery

A combination of satellite images from different sources (Fig. 5) was used to assess the impacts of September 2017 hurricanes on shoreline position. To have a reference state of the coastal system, and in the absence of a more recent image, as no significant wave event occurred between February and September, a pre-hurricane Pléiades image of 25 February 2017 (i.e. about 7 months before Irma) was used. In addition, a Pléiades image of 10 September 2017 was used to assess the post-hurricane situation. However, due to hurricane-induced cloud cover, the beaches of Flamands, Saint-Jean and Lorient were not treatable at the second date. To overcome this difficulty, we used a DigitalGlobe image of 13 September 2017, which was downloaded freely from Google Earth. All the images used in this study were high resolution, with a pixel size ranging from 0.2 m (DigitalGlobe) to 0.5 m (Pléiades). The specifications of satellite images are reported in Table 2. Multispectral Pléiades satellite images were pan-sharpened using the ENVI 5 software. This process merges a high-resolution panchromatic raster with a low-resolution multispectral raster that were captured simultaneously, providing high-resolution colour images that facilitate shoreline proxies' detection during digitization. Although the Pléiades image of 10 September 2017 was delivered georeferenced, it showed a horizontal offset with the image of 25 February 2017. Post-hurricane Pléiades (10 September 2017) and DigitalGlobe (13 September 2017) images were georeferenced in ArcGIS 10.5, using ground control points extracted from the pre-hurricane image of 25 February 2017. Images were rectified in the WGS 1984 UTM Zone 20N (EPSG: 32620) coordinate system using a projective transformation. On Saint-Barthélemy Island, the presence of many anthropogenic (e.g. jetties, roads) and natural features (e.g. headlands, beachrock) made this operation easier than on other less built or uninhabited tropical islands (e.g. atoll islands, Ford, 2013; Duvat and Pillet, 2017; Kench et al., 2018), which increased the georeferencing accuracy (Table 2).

Date	Image type	Pixel size (m)	Georeferencing error (m)
25 February 2017	Satellite (Pléaides-1A)	0.50	/
10 September 2017	Satellite (Pléiades-1B)	0.50	0.48
13 September 2017	Satellite (DigitalGlobe)	0.20	0.73

Table 2. Characteristics of the satellite images used in this study.

3.1.2. Shoreline interpretation and digitization

Since the use of one single proxy is insufficient to fully assess hurricane-induced changes caused to coastal systems (Duvat and Pillet, 2017; Duvat et al., 2017b, c), we used several complementary shoreline indicators. The seaward limit of the vegetation is the most commonly used shoreline indicator. It allows delineating the stable part of the coastal system in natural settings (Webb and Kench, 2010; Ford, 2012, 2013; Yates et al., 2013; Mann and Westphal, 2014; Ford and Kench, 2014, 2015; McLean and Kench, 2015; Mann et al., 2016; Kench et al., 2018). However, it excludes anthropogenic features, which are common in highly-developed settings. As these features can induce a stabilization of the shoreline, in line with previous studies (e.g. Duvat et al., 2016; Duvat et al., 2017c), we used the "stability line" (SL) instead of the "vegetation line" (VL) as a shoreline proxy (Fig. 4a, b, e). On natural coasts, the SL corresponds to the external limit of the vegetation (Fig. 4a), while on artificial coasts along which anthropogenic features (e.g. coastal defence structures, property walls) were built, the SL was digitized on the oceanward limit of these features (Fig. 4b). On the post-hurricane images, the SL was digitized excluding scattered vegetation remains and isolated plants. During the digitization, a particular attention was paid to avoid misinterpretation. Uprooted vegetation (excluded from the SL) could be confused with the vegetation that had resisted (included in the delineation of the SL). Moreover, the operator had to distinguish hurricane-driven debris accumulation from soil scouring. Field observations (notably geolocated ground photographs) and post-hurricane pansharpened satellite images helped the operator to digitize the SL and to avoid position errors.

As beaches are part of the sedimentary system, the base of the beach (BB) was also digitized (Rankey, 2011; Biribo and Woodroffe, 2013, Mann and Westphal, 2014; Duvat and Pillet, 2017; Duvat et al., 2017b, c). This proxy corresponds to the limit between the beach and the foreshore (Fig. 4c, d). It allows assessing the impacts of the hurricane waves on beaches, including changes in beach position and in beach area. The latter was obtained by merging the BB with the SL for the pre- and post-hurricane situations in ArcGIS. In places, the limit between the beach and the foreshore was not clearly detectable and the digitization required particular attention to avoid BB

misplacement. In this case, the visual appreciation of changes in sand density between the beach (higher density) and the foreshore (lower density) was used to differentiate the beach from suspended sediment. The BB was not digitized when uncertainty was high. Additionally, on some open beaches, wave breaking masked the BB, making impossible its digitization.

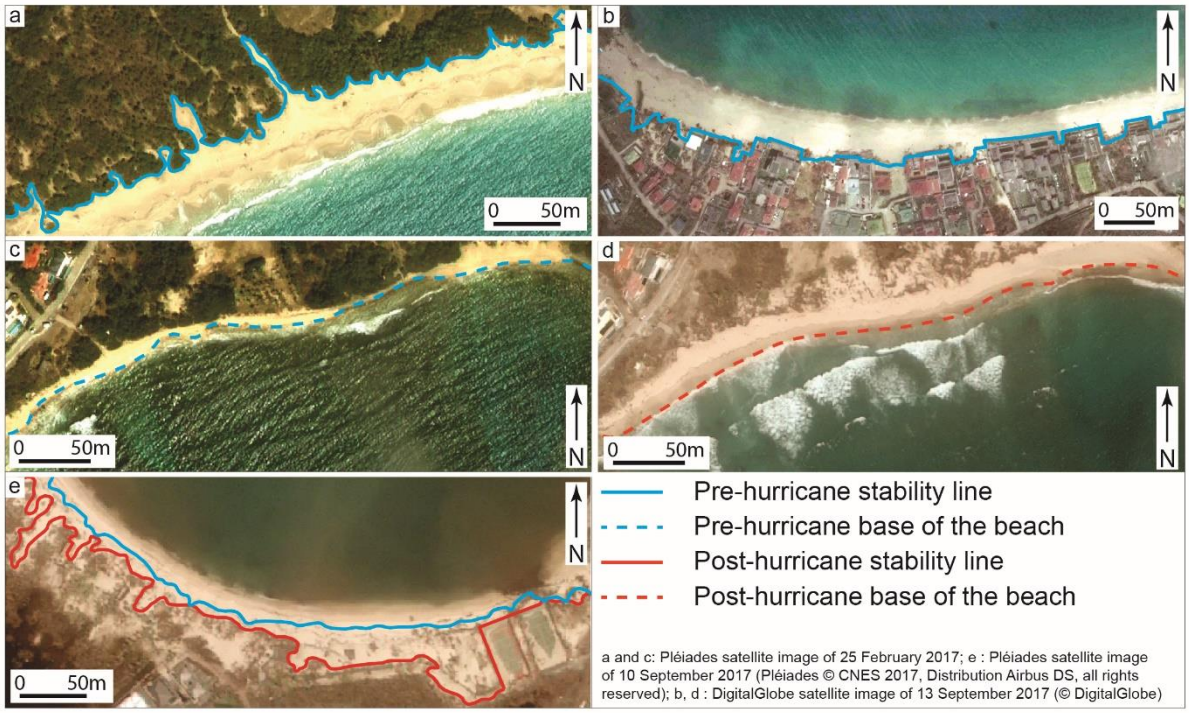

Fig. 4. Shoreline indicators used in this study. (a) shows the position of the pre-hurricane stability line on natural coasts (here, Grande Saline), where it corresponds to the seaward limit of the vegetation. (b) illustrates the digitization of the post-hurricane stability line on developed coasts (here, Flamands), where it corresponds to the external limit of human-built structures (i.e. seawalls, ripraps, buildings). (c) and (d) illustrate the pre- and post-hurricane positions of the base of the beach, respectively (here, at Toiny). (e) represents the position of the pre- and post-hurricane stability line.

3.1.3. Uncertainty

Shoreline change

Uncertainty related to shoreline digitization from aerial photographs and satellite imagery has already been the subject of several studies (Anders and Byrnes, 1991; Thieler and Danforth, 1994; Fletcher et al., 2003). As Ford (2012) mentions, five sources of uncertainty were identified by Fletcher et al. (2003): seasonal error, tidal fluctuation error, digitizing error, pixel error and rectification error. Because shoreline indicators used in this study were not influenced by the seasonal error, and very little influenced by the tidal fluctuation error (tidal height was

only 12 cm higher in September compared to February), in line with previous studies (Ford, 2012; Yates et al., 2013; Duvat and Pillet, 2017; Kench et al., 2018), we considered three error sources: rectification error (E_r), pixel error (E_p) and digitizing error (E_d). E_r corresponds to the offset between the satellite image used as a spatial reference (i.e. 25 February 2017 image) and the rectified images. It was calculated using random landmarks that can be easily detected on each image. Using the "Point Distance" tool in ArcGIS, we are able to estimate the mean offset between the spatial reference and rectified images (Table 3). E_p is equal to the pixel size (i.e. the image resolution) of the images used in this study (Table 2). The pixel size influences both images georeferencing and shorelines digitization accuracies. E_d corresponds to the uncertainty related to the digitization of shoreline proxies and it was estimated during the operation.

We only considered error related to rectified images. The mean rectification error was equal to 0.60 m (ranging from 0.48 m to 0.73 m). The mean pixel size error was 0.35 m. During the digitization process, the SL was easier to detect than the BB, due to active hydrodynamical conditions. As a result, we considered respectively an error <1 m for the SL and <3 m for the BB (Table 3). Consequently, the global uncertainty was considered to be <2 m for the SL and <4 m for the BB, making changes respectively <2 m (±2 m) and 4 m (±4 m) not significant (relative stability). Transects showing changes ≥ + 2 m and ≥ + 4 m, respectively, for the SL and BB, therefore indicate shoreline advance, while transects showing respective changes ≤– 2 m and ≤–4 m for these two shoreline proxies indicate shoreline retreat.

Image	Rectification error (m) (E_r)	Pixel error (m) (E_p)	Digitizing error (m) (E_d)	
			SL	BB
25 February 2017 Pléiades	0 (spatial reference)	0.50	1.00	3.00
10 September 2017 Pléiades	0.48	0.50	1.00	3.00
13 September 2017 DigitalGlobe	0.73	0.20	1.00	3.00
Mean error (m)	0.60	0.35	1.00	3.00

Table 3. Sources of uncertainty considered in this study and related error. Mean rectification error does not include the spatial reference.

Beach area uncertainty

In accordance with previous studies (Kench et al., 2015; Duvat et al., 2017b), only errors related to image resolution (0.35 m, Table 3) and shoreline digitization (1 m for the SL and 3 m for the BB, Table 3) were

considered when estimating changes in beach area. The rectification error was excluded, because it has no influence on surface calculation. Consistent with Duvat et al. (2017b), a buffer was calculated for each of the two shoreline proxies delimiting beaches (i.e. the SL and the BB) to calculate area uncertainty. The width of the buffer corresponds to the sum of the error values considered for each indicator. Consequently, buffers of 1.35 m (0.35 m + 1.00 m) and 3.35 m (0.35 m + 3 m) were created for the SL and the BB, respectively. The areas of these two buffers were then added to obtain the uncertainty area for each beach. For example, beach area uncertainty for Flamands equals the uncertainty related to the SL (0.10 ha) + uncertainty related to the BB (0.21 ha) = 0.31 ha.

3.1.4. Shoreline change analysis

Shoreline change was calculated using the Digital Shoreline Analysis System (DSAS), an extension in ArcGIS, which is commonly used to assess changes in shoreline position (Thieler et al., 2017). Perpendicular transects were generated every 10 m along a baseline that was digitized parallel to the shoreline. The Net Shoreline Movement (NSM), which corresponds to the distance between the oldest and the most recent shorelines, was generated automatically by DSAS for both the SL and BB.

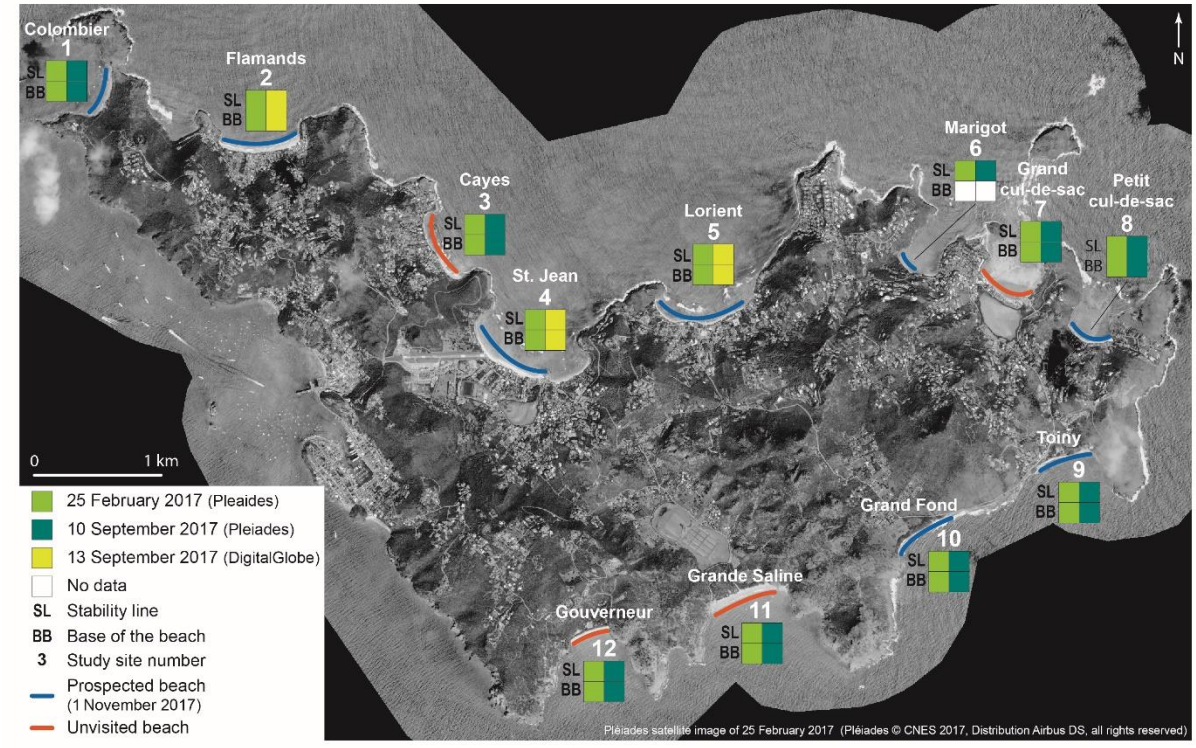

Fig. 5. Spatial extent of the satellite images used in this study. We were not able to digitize the base of the beach at Marigot due to wave breaking making it visually undetectable on images.

3.2. Assessment of hurricanes morphological impacts

Post-hurricane fieldwork completed on 1 November 2017 allowed assessing the erosional and accretional impacts of September 2017 hurricanes on beaches. Field observations mainly consisted of making an inventory of the features that were presumed to be hurricane-generated. The position of the cliffs cut by hurricane waves in upper beaches and sand dunes was geolocated, and their height was measured. As the field trip was conducted seven weeks after the hurricanes, the features observed in the active beach zone had already been reworked by waves. Likewise, as beach recovery had already started at the time of fieldwork, cliff height was considered to provide not a precise estimate of sediment ablation, but a useful indication of the intensity of wave impact. In addition, hurricane wreck lines and sediment deposits were mapped, and the thickness of the latter was measured. As hurricane-generated accretional features were mainly found out of the active beach zone, i.e. first, on the upper beach, and second, within a 30 m-wide coastal strip from the pre-hurricane vegetation line, they were generally intact at the time of the field visit, except where they had been removed or reworked by residents or by public authorities. We were therefore able to make a detailed description of these features. So as to collect additional information on hurricanes impacts (i.e. check the hurricane origin of observed deposits, collect the initial values of hurricane-induced beach lowering), we conducted interviews among present primary residents and private companies' employees recruited by residents to secure properties from burglary or to repair damages. Interviewees provided valuable complementary information on the immediate post-hurricane situation, and on the extent of sediment reworking and of beach readjustment at the time of the field visit.

3.3. Assessment of the impacts on and of the role of the coastal vegetation

Although the role of the coastal vegetation is rarely considered in geomorphic studies, some previous assessments highlighted that a well-preserved indigenous vegetation belt reduces the erosional and destructive impacts of hurricanes on coastal systems (i.e. beach-dune systems and barrier beaches) and human assets (e.g. buildings, roads…) respectively, through the attenuation of wave energy and sediment trapping (Stoddart, 1963, 1965; Duvat et al., 2016; Duvat et al., 2017b). While wave attenuation by the indigenous vegetation reduces the damages caused to human assets by waves and thrown coral debris, sediment trapping by the dense branch and root system of this vegetation contributes to the development (i.e. widening and gain in elevation) of the beach ridge. In the long run, beach ridge development diminishes the risk of flooding. On the contrary, these studies showed that where the indigenous vegetation had been replaced by introduced vegetation (e.g. coconut trees), both the erosional and destructive impacts of waves were higher, while the abovementioned constructional processes were not observed. Such observations justify including the analysis of the nature and role of the coastal vegetation in hurricane impact assessments.

Accordingly, using pre-hurricane satellite imagery and ground photographs taken in 2007 by one of the authors who had already completed beach surveys on the island, we identified the main shrubby and wooded species growing on the upper beach, on sand dunes, and in inner land areas within a 30 m-wide coastal strip from the vegetation line. The freely available DigitalGlobe satellite images provided by Google Earth (which date back to 28/11/2003) were used to check that the vegetation had not changed between the field visit of 2007 and 2017. Based on this assessment, we classified the coastal vegetation into three distinct categories, namely predominantly indigenous, predominantly introduced, and mixed. Given the relative homogeneity of the coastal vegetation on the scale of beach sites, we did not make within-site distinctions. The destructive impacts of hurricane waves and wind on the coastal vegetation growing within a 30 m-wide coastal strip extending inland from the pre-hurricane vegetation line were assessed. These impacts were characterized (i.e. uprooting, trunk and branch breaking, etc.) and geolocated for each vegetation type (shrubby vs. wooded) and species affected. Additionally, the role of the coastal vegetation in buffering the impacts of hurricane waves was assessed, based on the collection of field observations on *(i)* the extent of surface erosion in and out of vegetated areas, according to vegetation type (i.e. indigenous, introduced or mixed), *(ii)* the landward extent of hurricane-induced deposits, depending on vegetation occurrence and type, and *(iii)* sediment trapping (measurement of the thickness of deposits, depending on vegetation occurrence and type).

3.4. Assessment of the influence of human-built structures on beach response

3.4.1. Assessment of the natural vs. artificial character of the shoreline

The stability line (SL) was classified into two categories. SL sections with and without human-built structures, i.e. coastal protection structures such as seawalls or ripraps and alongshore buildings, were respectively classified as artificial and natural. In the former case, the SL corresponds to the vegetation line (Fig. 6a, b), while in the latter case it corresponds to the base of human-built structures (Fig. 6c, d). This classification was adopted to allow the analysis of the SL response to the hurricane waves depending on its nature (i.e. natural vs. artificial). The nature of the SL was assessed using the satellite image of 25 February 2017 and the ground photographs taken in the field in 2007 by one of the authors, which helped identifying human-built structures in areas exhibiting no change since 2007. Likewise, the same classification was applied to the post-hurricane SL using the images of 10 September 2017 and 13 September 2017, and geolocated ground photographs of 1 November 2017. This allowed estimating changes in the nature of the shoreline.

3.4.2. Assessment of the influence of "coastal squeeze" on beach response

The seaward limit of the built environment, i.e. of the built area located in the coastal zone at a certain distance from the SL, was digitized in order to allow distinction between shoreline sections still having a natural buffering, i.e. non-built, area between the active beach zone and coastal human assets, and shoreline sections affected by "coastal squeeze" (Cooper and McKenna, 2008; Cooper and Pile, 2014), i.e. exhibiting no if a very narrow natural buffering area as a result of extensive urbanization (Fig. 6e). The digitization of the seaward limit of the built environment was completed using the post-hurricane images of 10 and 13 September 2017, on which this limit was made easily detectable by vegetation destruction. The distance between the pre-hurricane SL and the limit of the built environment (Fig. 6e) was calculated using DSAS software in ArcGIS 10.5 (SCE), using the same transects that were used to measure changes in shoreline position. This allowed analyzing the influence of variations in the width of the natural buffering area on beach response.

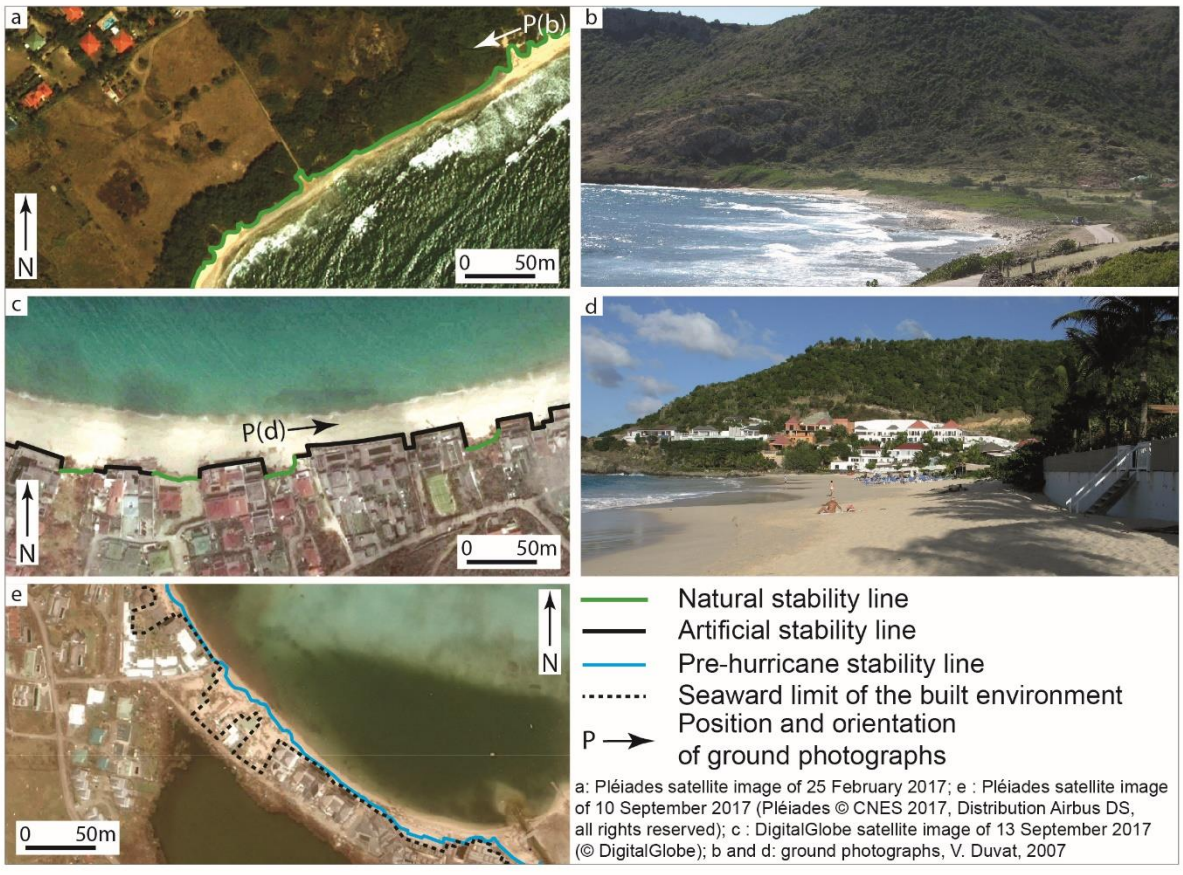

Fig. 6. Indicators used in this study to assess the contribution of longitudinal human constructions to beach response. (a) illustrates pre-hurricane 'natural' stability line. In this case, no human-built structure was present, as shown on photograph (b) (Grand Fond). (c) shows the alternation of artificial and natural stability line sections in

the post-hurricane situation (Flamands). (d) shows, in the foreground, longitudinal coastal structures (here, a private property wall), and in the background, a vegetated shoreline section, which respectively illustrate artificial and natural shoreline sections. (e) shows in dotted line the position of the seaward limit of the built environment as it was digitized on the post-hurricane image. The blue line represents the pre-hurricane stability line.

3.4.3. Uncertainty related to human-built structures detection

Uncertainty related to the digitization of the seaward limit of human-built structures was influenced by the capacity of the operator to detect these structures based on image interpretation. On pre-hurricane images, this limit was easily detectable on those sites having a limited vegetation cover, while it was generally masked by the vegetation where the latter was dense. In this case, wherever possible (i.e. where human-built structures had not been destroyed by the hurricane waves), we used post-hurricane images, on which vegetation destruction made them visible, to digitize their seaward limit. Where post-hurricane images could not be used to digitize human-built structures (i.e. where these structures had been either partly, or entirely damaged by the hurricane waves), field observations were used to determine their pre-hurricane seaward limit.

3.4.4. Statistical attribution of the influence of human-built structures

In order to quantitatively attribute the influence of human-built structures on the stability line response, several hypotheses have been formulated and tested using the dataset generated using R software (Table 4). Once produced, data related to the SL response (i.e. Net Shoreline Movement), the nature of the SL in the pre- and post-hurricane situations (i.e. natural vs. artificial) and the width of the natural buffering area (i.e. distance that separates the pre-hurricane SL from seaside human-built structures) , were spatially joined to the transects generated by the extension DSAS in ArcGIS, allowing statistical analysis on 561 observations (corresponding to the transects for which data are available). Table 4 summarizes the four hypotheses and the data used for the correlation tests.

Hypothesis	Data used to test the hypothesis
1 - Shoreline behaviour was strongly influenced by the nature of the pre-hurricane stability line (SL)	- Nature of the pre-hurricane SL (natural or artificial) - Shoreline change data (Net Shoreline Movement)
2 - The proximity of longitudinal structures to the SL had an influence on the SL response	- Width of the natural buffering area (distance between the pre-hurricane SL and the limit of the built environment) - Shoreline change data (Net Shoreline Movement)
3 - The SL response was strongly influenced by the longitudinal structures located within a 30m-wide coastal strip from the pre-hurricane SL	- Transects corresponding to artificial shoreline within a 30 m-wide coastal strip from the pre-hurricane SL - Shoreline change data (Net Shoreline Movement)

4 - The proximity of the longitudinal structures to the SL influenced changes in SL type, i.e. increased the extent of artificial shoreline, in the post-hurricane situation	- Transects corresponding to natural and artificial shoreline in the pre- and post-hurricane situations

Table 4. Hypotheses and data used to attribute the response of the stability line to human-built structures.

4. Results

4.1 Hurricanes impacts on shoreline position

4.1.1 Impacts on stability line position

At all study sites, September 2017 hurricanes caused a marked retreat of the stability line (SL) (Table 5 and Fig. 7). Depending on beach sites, the retreat of the stability line was detected along 47.73% (Lorient) to 100.00% (Marigot and Grand Fond) of transects. On 9 beaches (Flamands, Cayes, Saint-Jean, Marigot, Petit Cul-de-Sac, Toiny, Grand Fond, Grande Saline and Gouverneur) out of 12, more than 75% of transects exhibited retreat (Table 5, Fig. 7). The mean shoreline movement ranged from −2.76 m in the west of the island (Colombier) to −18.39 m in the south-east (Grand Fond) (Table 5). Six beaches out of 12 had an average retreat value exceeding −10 m. The highest average retreat values were recorded first, in the south-east (Grand Fond, −18.39 m; Toiny, −15.01 m) and north-east (Marigot, −13.98 m; Petit Cul-de-Sac, −12.43m), and second, on the northern coast of the island (Cayes, −16.01 m) (Table 5). The beach of Gouverneur, in the south, had a mean retreat value of −11.52 m. The lowest minimum NSM values respectively reached −50.76 m, −37.85 m, −34.82 m, −45.52 m, −61.82 m and −45.62 m, at Grand Fond, Toiny, Marigot, Petit Cul-de-Sac, Cayes and Gouverneur. The sites that were less affected (i.e. those with an average retreat value greater than −10 m, Table 5) however exhibited localized high retreat values. For example, Grand Cul-de-Sac (mean NSM, −6.66 m) had a minimum NSM value of −40.63 m. The highest minimum NSM value (−17.86 m) was obtained in the west of the island, at Colombier (Table 5, Fig. 8). The results thus show a high spatial variability of the SL response to the hurricane waves, with higher retreat values on the highly-exposed eastern and northern coasts, compared to the more sheltered southern and the western coasts (Table 5, Fig. 8).

Beach number and name	Number of transects	Mean NSM (m)	Min. NSM (m)	Max. NSM (m)	Accretional transects		Stable transects		Erosional transects	
					Nb	%	Nb	%	Nb	%
1. Colombier	25	−2.76	−17.86	0.00	0	0.00	13	52.00	12	48.00
2. Flamands	54	−8.99	−22.16	−0.57	0	0.00	9	16.67	45	83.33
3. Cayes	52	−16.01	−61.82	0.00	0	0.00	3	5.77	49	94.23
4. Saint-Jean	57	−9.15	−29.74	0.00	0	0.00	14	24.56	43	75.44
5. Lorient	88	−4.46	−22.55	0.00	0	0.00	46	52.27	42	47.73
6. Marigot	18	−13.98	−34.82	−2.64	0	0.00	0	0.00	18	100.00
7. Grand Cul-de-Sac	50	−6.66	−40.63	0.00	0	0.00	22	44.00	28	56.00
8. Petit Cul-de-Sac	37	−12.43	−45.52	0.00	0	0.00	3	8.11	34	91.89
9. Toiny	41	−15.01	−37.85	0.00	0	0.00	4	9.76	37	90.24
10. Grand Fond	49	−18.39	−50.76	−4.77	0	0.00	0	0.00	49	100.00
11. Grande Saline	58	−7.64	−34.02	0.00	0	0.00	13	22.41	45	77.59
12. Gouverneur	32	−11.52	−45.62	−1.02	0	0.00	2	6.25	30	93.75

Table 5. Change in the position of the stability line between February 2017 and September 2017.

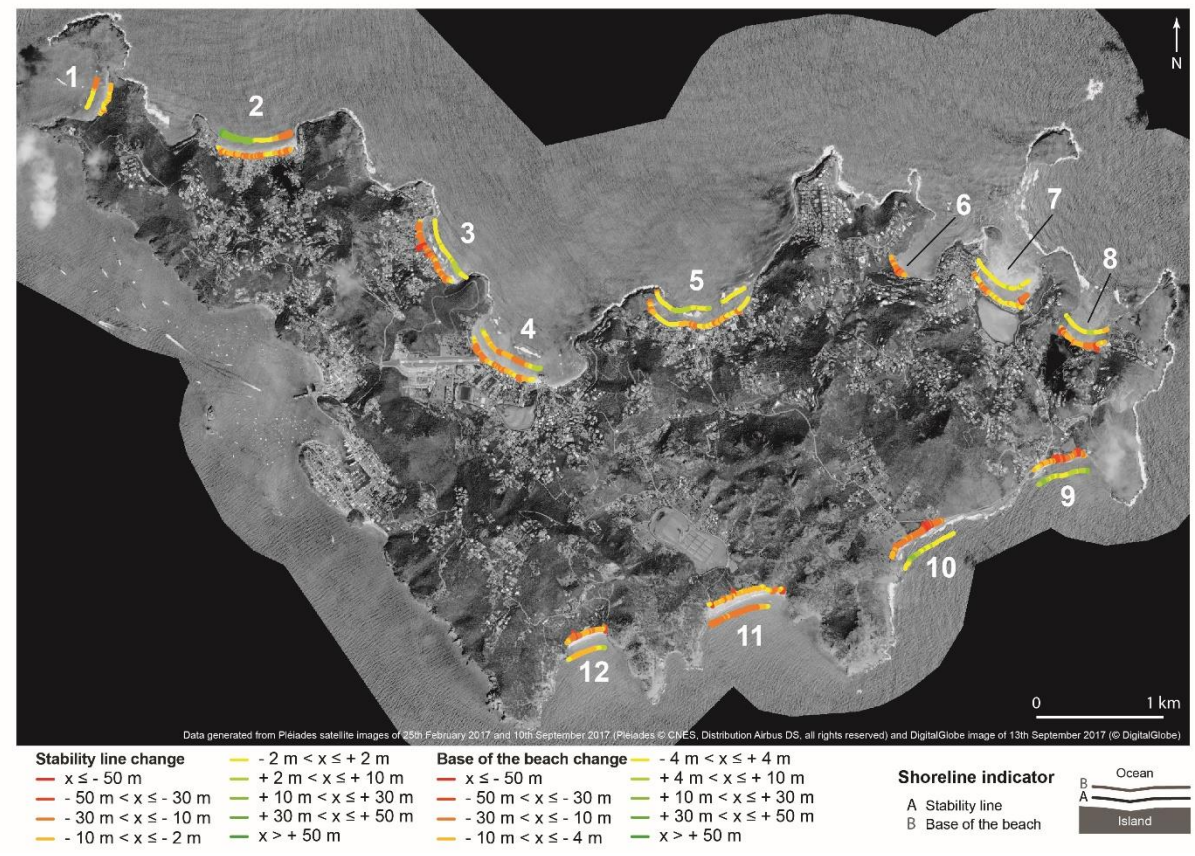

Figure 7 – Inferred impacts of September 2017 hurricanes on shoreline position on Saint-Barthélemy Island. This figure highlights first, the spatial variability of the stability line response on the island scale, depending on site exposure to the hurricane waves, and second, the contrasting behaviours of the stability line (predominantly showing retreat) and of the base of the beach (mainly exhibiting either stability, or retreat).

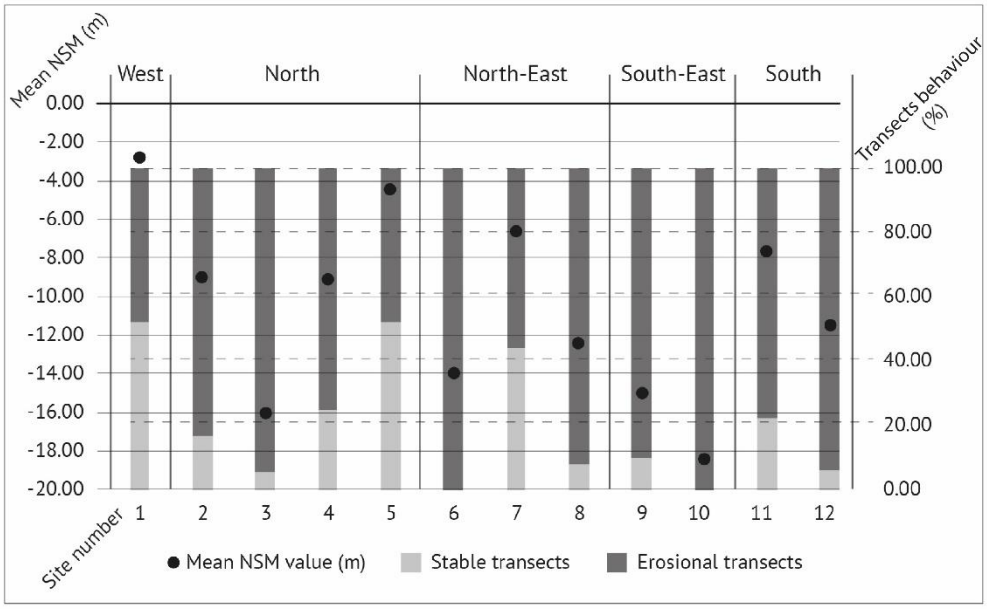

Fig. 8. Summary of the stability line response on Saint-Barthélemy.

4.1.2 Impacts on the position of the base of the beach

As a reminder, changes in the position of the base of the beach (BB) were assessed on all beaches except Marigot. On the island scale, the response of the BB varied significantly (Figure 7). Four sites out of 11 predominantly showed a retreat of the BB. For example, in the south, Grande Saline exhibited 93.75% of retreating transects, with respectively mean and minimum NSM values of −14.61 m and −24.76 m (Table 6). Likewise, Saint-Jean in the north and Gouverneur in the south respectively had 68.52% and 67.75% of retreating transects, with mean and minimum NSM values reaching −5.11 m and −16.52 m, and –4.45 m and −9.77 m, respectively (Table 6). In contrast, the BB was predominantly stable on 6 sites (Colombier, Cayes, Lorient, Grand Cul-de-Sac, Petit Cul-de-Sac, Grand Fond), with 64.00% (Colombier) to 93.75% of stable transects, depending on sites (Table 6). For example, at Colombier, the mean and minimum NSM values reached −4.36 m and −15.42 m, respectively. Noteworthy, the BB showed advance on 2 sites out of 11, i.e. Flamands in the north (mean NSM, +5.56 m) and Toiny in the south-east (mean NSM, +6.31 m). Flamands exhibited high alongshore variability, with 48.14% of accretional transects, 25.93% of stable transects and 25.93% of eroding transects. Furthermore, we observe a high variability in the behaviour of the BB between the western and eastern parts of the beach (Figure 7). On this beach, the maximum NSM value was recorded in the west (+35.86m), while the minimal NSM value was found in the east (−26.70m) (Table 6). In the south-east, at Toiny, accretion was detected along 73.17% of transects, while no transect retreated. On this beach, mean NSM reached +6.31 m (Table 6).

Beach number and name	Number of transects	Mean NSM (m)	Min. NSM (m)	Max. NSM (m)	Accretional transects		Stable transects		Erosional transects	
					Nb	%	Nb	%	Nb	%
1. Colombier	25	−4.36	−15.42	3.63	0	0.00	16	64.00	9	36.00
2. Flamands	54	5.56	−26.70	35.86	26	48.14	14	25.93	14	25.93
3. Cayes	52	2.89	−0.02	9.92	13	25.00	39	75.00	0	0
4. Saint-Jean	54	−5.11	−16.52	8.32	8	14.81	9	16.67	37	68.52
5. Lorient	68	2.20	−11.63	7.41	19	27.94	47	69.12	2	2.94
6. Marigot	N.D.	N.D.	N.D.	N.D.	N.D.	N.D.	N.D.	N.D.	N.D.	N.D.
7. Grand Cul-de-Sac	48	0.67	−1.61	6.14	3	6.25	45	93.75	0	0.00
8. Petit Cul-de-Sac	37	0.15	−5.97	6.22	6	16.22	28	75.68	3	8.10
9. Toiny	41	6.31	1.99	14.16	30	73.17	11	26.83	0	0.00
10. Grand Fond	49	2.43	−3.90	12.14	15	30.61	34	69.39	0	0.00
11. Grande Saline	48	−14.61	−24.76	−2.52	0	0.00	3	6.25	45	93.75
12. Gouverneur	31	−4.45	−9.77	6.14	4	12.90	6	19.35	21	67.75

Table 6. Change in the position of the base of the beach between February 2017 and September 2017. N.D.: No Data

4.1.3 Changes in beach area

On the island scale, 8 beaches (Flamands, Cayes, Lorient, Grand Cul-de-Sac, Petit Cul-de-Sac, Toiny, Grand Fond and Gouverneur) out of 11 expanded, with rates of change ranging from +62.32% (Flamands, north) to +251.35% (Toiny, south-east) (Table 7), while 2 beaches (Colombier and Saint-Jean) were stable in area and only one beach (Grande Saline) contracted. The most common mode of expansion, recorded on 4 beaches (Cayes, Lorient, Grand and Petit Cul-de-Sac), resulted from the retreat of the SL, while the BB was stable. For example, Cayes Beach expanded by +227.08%, with a net surface gain of +1.09 ha. Two beaches, i.e. Flamands and Toiny, expanded as a result of the retreat of the SL combined with an advance of the BB. On these sites, the beach area increased respectively by +66.32% and +251.35% (Table 7). At Gouverneur, the retreat of both the SL and the BB caused an increase of +33.87% in the beach area (Table 7). In contrast, Grande Saline was the only beach that contracted (-0.40 ha, representing a beach area loss of -20.73%), mainly due to the marked retreat of the BB. Of note, the beach area of Colombier and Saint-Jean was stable (Table 7).

Beach number and name	Pre-hurricane area (ha)	Post-hurricane area (ha)	Area uncertainty		Net land area change (ha)	Evolution (%)	Beach response
			ha	%			
1. Colombier	0.49	0.44	0.14	28.20	−0.05	−10.20	Stability
2. Flamands	1.38	2.24	0.31	22.59	+0.86	+62.32	Expansion
3. Cayes	0.48	1.57	0.29	60.78	+1.09	+227.08	Expansion
4. Saint-Jean	1.21	1.51	0.36	29.95	+0.30	+24.79	Stability
5. Lorient	0.53	1.08	0.41	76.56	+0.55	+103.77	Expansion
6. Marigot	/	/	/	/	/	/	/
7. Grand Cul-de-Sac	0.57	0.94	0.28	49.10	+0.37	+64.91	Expansion
8. Petit Cul-de-Sac	0.45	1.09	0.20	43.65	+0.64	+142.22	Expansion
9. Toiny	0.37	1.30	0.22	58.64	+0.93	+251.35	Expansion
10. Grand Fond	0.52	1.61	0.26	49.77	+1.09	+209.62	Expansion
11. Grande Saline	1.93	1.53	0.35	18.09	−0.40	−20.73	Contraction
12. Gouverneur	0.62	0.83	0.17	26.69	+0.21	+33.87	Expansion

Table 7. Changes in beach area between February 2017 and September 2017. Beach area was calculated using the stability line as the landward boundary and the base of the beach as the oceanward limit of beaches.

4.2. Hurricanes impacts on coastal morphology

The hurricanes had both erosional and accretional impacts. Erosional features were predominant, and detected along most beaches. However, they showed variations, both in nature and in extent, between beach sites. On the fore beach, rock formations were revealed by sediment loss, as at Colombier where the retreat of the BB caused the emergence of beachrock slabs, especially at its northern extremity (Fig. 9a). In addition, beach lowering was widespread along longitudinal constructions, detected at Flamands, Lorient and Marigot. In front of human constructions, such as houses' seaside retaining walls, the highest values of beach lowering reached up to −2.00 m at Flamands (Fig. 9b). On other densely urbanized sites, lower values were recorded, as illustrated by Lorient, where beach lowering reached 0.60 m (Fig. 9c). Generally, beach lowering revealed the foundations of longitudinal structures that were previously masked by sediment. In contrast, on natural beaches, beach lowering exhibited lower values, i.e. ranged from 0.20 m (e.g. Petit Cul-de-Sac, Fig. 9d) to 0.60 m (e.g. Grand Fond). Moreover, the hurricane waves cut cliffs in upper beaches and sand dunes. Where the latter occur (Flamands, Saint-Jean, Grand Fond), erosion scarps locally reached up to 3.50 m in height (e.g. Flamands, Fig. 9e). Conversely, where beaches are backed onto a low-lying coastal plain, erosion scarps were much lower, e.g. from 0.40 m to 0.60 m high at Grand Fond (Fig. 9f).

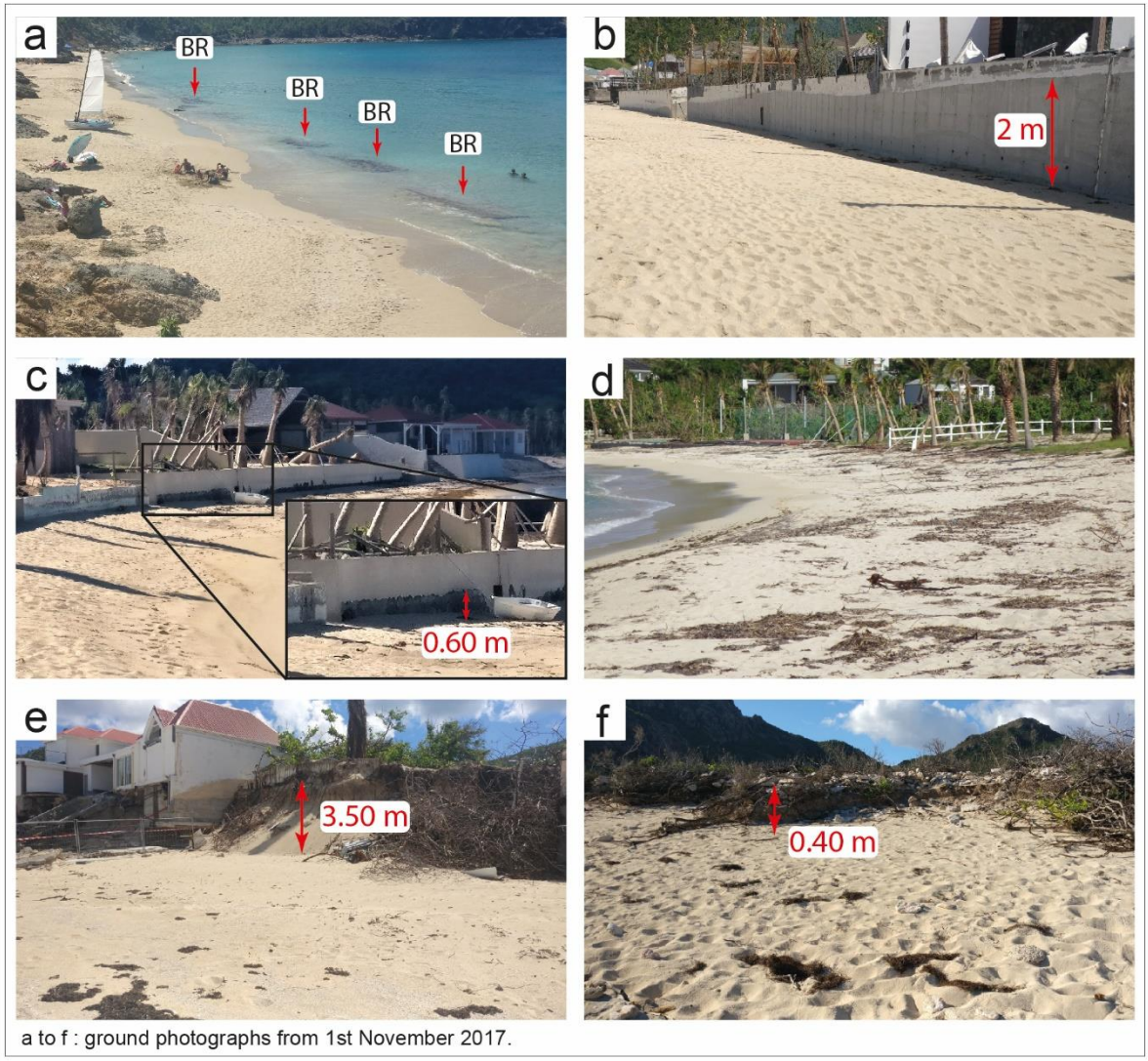

Fig. 9. Inferred erosional impacts of September 2017 hurricanes on Saint-Barthélemy Island. (a) shows the beachrock slabs revealed by sediment loss, here at Colombier. (b) and (c) illustrate beach lowering in front of longitudinal structures in densely urbanized areas, respectively at Flamands and Lorient. (d) illustrates beach lowering at a natural site, Petit Cul-de-Sac, where it rarely exceeded 0.20 m. (e) Post-hurricane cliff cut in the sand dune at Flamands. The marks on the nearby wall (at the background) indicate the previous extent of the dune. (f) cliff height was logically much lower on beaches backed onto a low-lying coastal plain, as illustrated here by Grand Fond.

The post-hurricane field survey also allowed assessing hurricane-induced accretional features, which could not be derived from image analysis. Most of the depositional features occurred on upper beaches and in inner land areas. On the former, where the indigenous vegetation was still in place, sediment deposits were noted, e.g. at Marigot, Grand Cul-de-Sac, Petit Cul-de-Sac, Toiny and Grand Fond. At Grand Fond, these deposits were composed of

coral rubble and blocks having dimensions of 0.10 to 0.30 m X 1 m (Fig. 10a). On the other sites, these depositional features were mainly composed of sand. Additionally, hurricane waves and winds deposited significant volumes of sand and coral debris in inner land areas, notably at Petit Cul-de-Sac and Toiny. At Toiny, overwash processes led to the formation of coral sand sheets extending inland as far as 45 m from the pre-hurricane vegetation line. As shown on Fig. 10 b and c, the debris almost reached the back-beach lagoon at Toiny. On urbanized beaches, inland sediment deposition mainly occurred in the axis of beach accesses and where the indigenous vegetation had been removed. At Saint-Jean, the easternmost part of the airstrip was covered by thin sand deposits. Accretional features occurring in the beach area were only observed at Grand Fond. At the eastern end of this beach, a 1.50 m-high and 100 m-long rubble ridge formed, composed of reworked smooth coral debris having a diameter ranging from 5 to 20 cm (Fig. 10d).

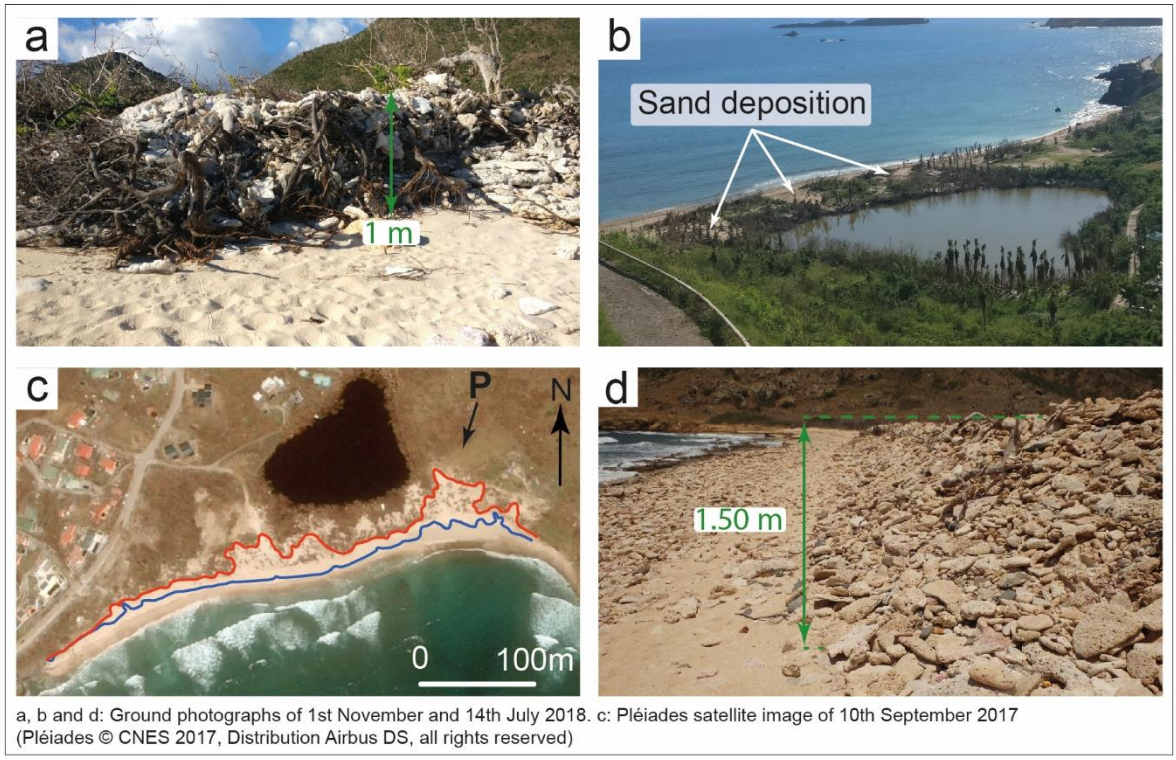

Fig. 10. Inferred accretional impacts of September 2017 hurricanes on Saint-Barthélemy Island. (a) illustrates the role of the indigenous vegetation in sediment trapping, which caused the vertical accumulation of sand and coral debris, here at Grand Fond. (b) illustrates sediment deposition due to the overtopping of the barrier beach of Toiny. (c) illustrates the position of the pre- (blue line) and post-hurricane (red line) stability line on the barrier beach of Toiny. While the stability line retreated, inner land areas increased in height as a result of sediment inputs. The

black arrow shows the position and orientation of ground photograph (b). (d) shows a coral rubble ridge composed of smooth coral debris at the eastern end of Grand Fond.

4.3 Influence of human disturbances on shoreline response

4.3.1 Impacts of vegetation modification on shoreline and beach response

As a reminder, on most beaches (e.g. Flamands, Cayes, Saint-Jean, Lorient, Marigot, Grand Cul-de-Sac, Toiny, Grande Saline and Gouverneur; see Table 1), tourism development and urbanization had led to the clearing or removal of the coastal indigenous vegetation. Despite shoreline retreat was observed along all natural shoreline sections (Table 5), where the indigenous vegetation had been preserved, it buffered the impacts of hurricane waves. While the first vegetation line (over a distance of 10 to 30 m) suffered significant damage (e.g. uprooting, trunks and branches breaking, salt-burning of leaves), the remaining vegetation promoted sediment trapping, which allowed the vertical accretion of the upper beach and of inland areas (e.g. Grand Fond, Fig. 10a and d). As a result of the buffering role of the indigenous vegetation, flooding and the deposition of sand and coral debris inland was limited.

4.3.2 Impacts of longitudinal structures on beach response

On the island scale, the SL response was highly influenced by the degree of shoreline hardening (Fig. 11, bar 3, pre-hurricane). Image analysis and field observations show a net contrast between natural and artificial shoreline behaviour (Figs. 11, 12 and 13). First, as shown in Figure 13a, natural shoreline mainly exhibited retreat. Retreat values range from 0 to –60 m, with 50% of the values falling between −5 and −15 m. In contrast, artificial shoreline underwent limited retreat (50% of the armoured shoreline have NSM values equal to 0), due to the resistance of most longitudinal structures and buildings to the hurricane waves. The beach sites of Cayes, Saint-Jean, Lorient and Grand Cul-de-Sac illustrate this latter situation, with NSM values ranging from 0 m to −2 m only (Fig. 11, see bars 2 and 3, pre-hurricane). Where the longitudinal structures were destroyed by the hurricane waves, higher retreating values were obtained, as along Flamands and Saint-Jean beaches (Fig. 11, see bars 2 and 3, pre-hurricane, from transect 51). Such situations correspond to the extreme values shown in Figure 13a for artificial shoreline. Second, the pre-hurricane width of the natural buffering area (extending seaward from the built area) influenced the extent of the SL retreat, as shown by the correlation in Figure 13b. Moreover, as shown in Figure 13c, the presence or absence of longitudinal structures within the 30 m-wide coastal strip highly influenced the response of the SL. While the values of SL retreat are widely scattered, showing no specific response pattern (i.e. Kendall's rank correlation tau = −0.39 and p-value < 3.62e-11), where no longitudinal structures were present in

this area, we observe a direct relationship expressed by a correlation between the proximity of the longitudinal structures and shoreline change values where these structures were present (Fig. 13c, artificial shoreline). Furthermore, the Kendall's rank correlation tau, which measures the correlation between two variables (see Table 4, hypothesis 3), is equal to −0.84, reflecting a strong significant relationship with a p-value < 0.05 (p-value < 2.2e-16).

On urbanized beaches (e.g. Flamands, Cayes, Saint-Jean, Lorient and Grand Cul-de-Sac), human-built structures located at a distance smaller than 30 m from the pre-hurricane SL thus limited the retreat of the SL. However, at these sites, because of the destruction of the coastal vegetation that constituted a buffer between these structures and the beach prior to the hurricane, the shoreline changed from natural before the hurricanes to artificial after these events (Fig. 13d). As a result, the length of artificial shoreline increased, as highlighted by the most illustrative examples, i.e. Flamands (from 6.72% to 63.2%; Fig. 11, bar 2) and Cayes (from 9.61% to 34.70%; Fig 11, bar 3). Collectively, these results highlight that the longitudinal structures built within a 30 m-wide coastal strip not only, influenced the response of the SL to the hurricane waves, but also and most importantly contributed to a change in the nature of the shoreline, from natural before the hurricanes to artificial after these events. The field survey conducted after the hurricanes showed that longitudinal structures strongly influenced erosional and accretional processes. As previously mentioned, beach lowering was greater in front of longitudinal structures (reaching up to –2 m at Flamands) due to wave reflection, compared to unbuilt vegetated areas, where it rarely exceeded −0.20 m (e.g. Petit Cul-de-Sac). Longitudinal structures also prevented sediment deposition on upper beaches and in inner land areas, except in the axis of beach accesses (e.g. Saint-Jean, Lorient and Grand Cul-de-Sac) or in localized open areas (e.g. Saint-Jean airstrip). By exacerbating the erosional and annihilating the accretional impacts of the September 2017 hurricanes on beaches, the longitudinal structures have contributed to a decrease in their sediment budget.

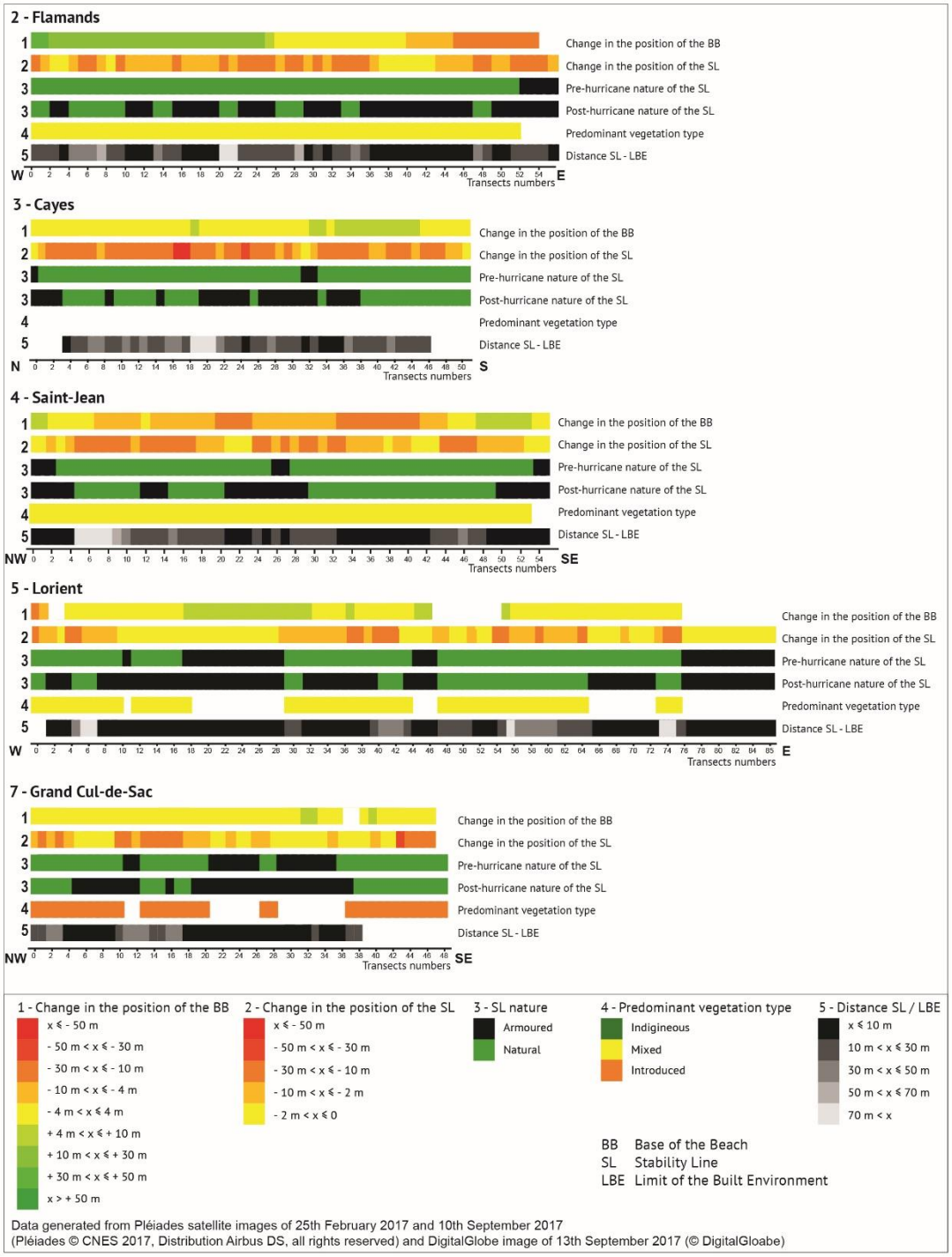

Fig. 11. Summary of shoreline changes inferred from September 2017 hurricanes on urbanized beaches of Saint-Barthélemy Island. Bars 1 and 2 show changes in the position of shoreline indicators, i.e. the base of the beach (1), and stability line (2). Bar 3 provides information about the SL nature (i.e. armoured vs. natural) for the pre- and post-hurricane situations. Bar 4 illustrates the vegetation type of natural sections for the pre-hurricane stability line. Bar 5 indicates the distance between the pre-hurricane stability line and the limit of the built environment, which corresponds to the width of the natural buffering area.

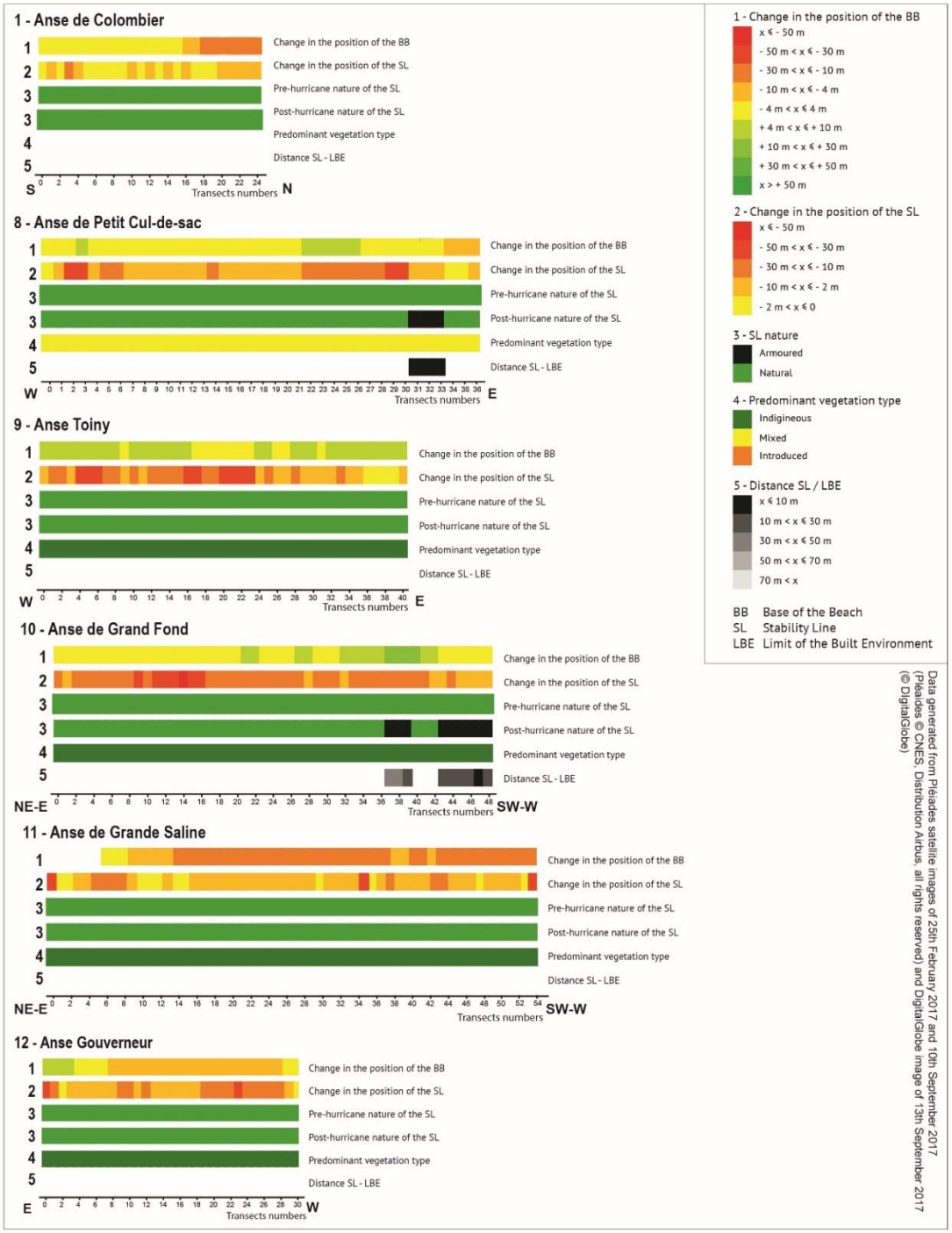

Fig. 12. Summary of shoreline changes inferred from September 2017 hurricanes on natural to little developed beaches of Saint-Barthélemy Island. Bar 1 and 2 show changes in the position of shoreline indicators, i.e. the base of the beach (1), and stability line (2). Bar 3 provides information about the SL nature (i.e. armoured vs. natural) for the pre- and post-hurricane situations. Bar 4 illustrates the vegetation type for natural sections of the pre-hurricane stability line. Bar 5 indicates the distance between the pre-hurricane stability line and the limit of the built environment, which corresponds to the width of the natural buffering area. Where no distance is indicated,

no human structure was present on the back beach. Here, only the sites of Petit Cul-de-Sac and Grand Fond were urbanized.

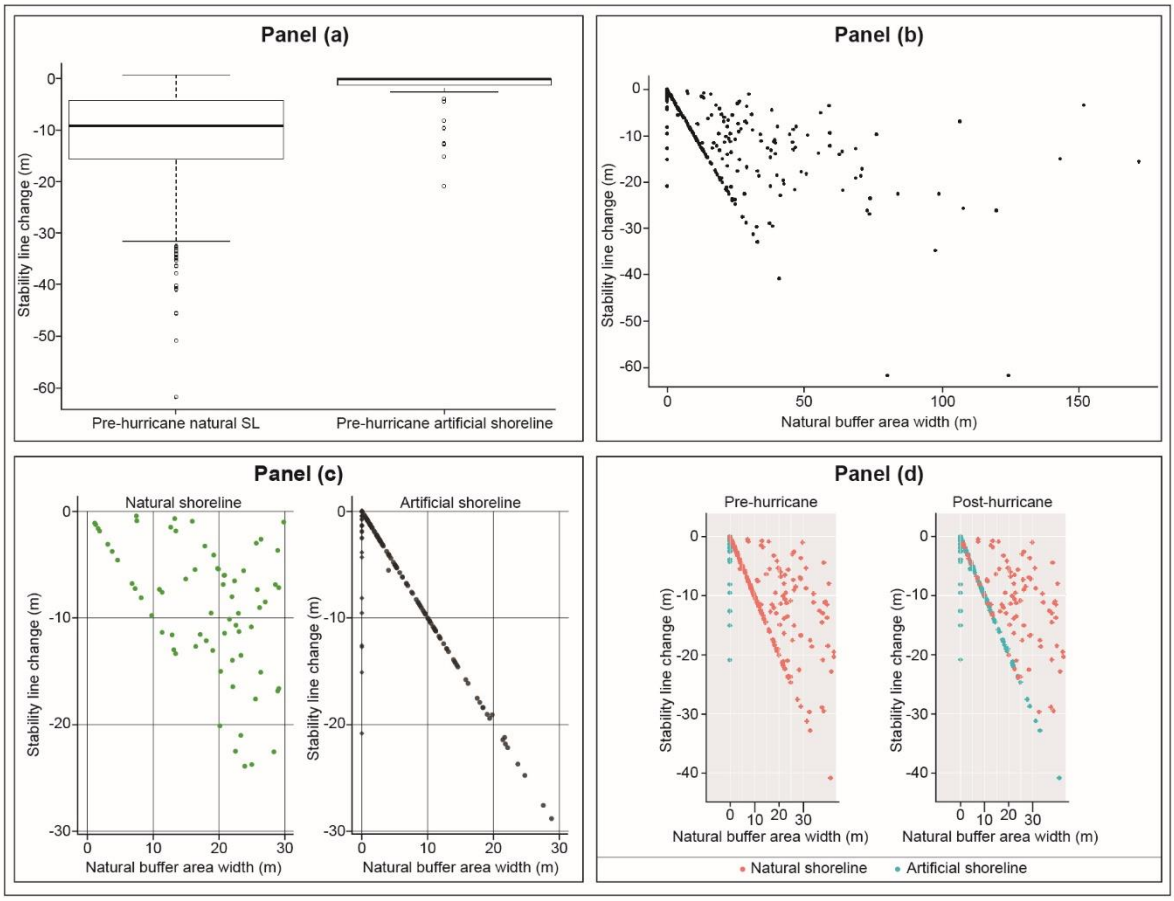

Fig. 13. Statistical analysis conducted to assess the influence of human-built structures on beach response. Panel (a) illustrate the contrasting response of the SL depending on its pre-hurricane nature (i.e. natural vs. artificial). Panel (b) shows that the width of the natural buffering area strongly influenced the extent of the SL retreat, especially where the presence of longitudinal structures was detected within a 30 m-wide coastal strip, for which a strong correlation was found (Panel c, Kendall's rank correlation tau = −0.84). Panel (d) shows that the length of hardened shoreline (blue dots) had increased after hurricanes, in response to the destruction of the narrow natural buffering area located in front of longitudinal coastal structures that were built within a 30 m-wide coastal strip (see SM1).

5. Discussion

5.1. Drivers of the spatial variability of shoreline and beach response

In line with previous studies (Cambers, 2009; Ford and Kench, 2014; Duvat et al., 2016), the results obtained emphasize the high spatial variability of shoreline and beach response under cyclonic conditions. Furthermore, they confirm that both natural and anthropogenic features play a major role in the response of a sedimentary system

to TCs (Stoddart, 1963, 1965; Bush, 1991; Scoffin, 1993; Cambers, 2009; Duvat et al., 2016; Duvat et al., 2017b). More precisely, we found that the two major drivers of the spatial variability of shoreline and beach response to the September 2017 hurricanes on Saint-Barthélemy were beach exposure and anthropogenic disturbances, the combined influence of which is shown in Figure 14.

First, beach exposure, which is directly determined by the hurricane's track and the surrounding morphological settings (i.e. presence of rocky headlands or of a fringing reef), was found to be a major driver of the spatial variability of impacts. The influence of this driver was noted at two different scales, that is, the island and the beach scales. On the island scale, shoreline change analysis showed that the highly-exposed eastern and northern beaches, where wave height reached and probably exceeded 10 m (Fig. 3), exhibited the higher mean NSM retreat values (i.e. Grand Fond, −18.39 m; Toiny, −15.01 m; Cayes, −16.01 m, for the SL), while the western and southern beaches (where wave height only reached 2-3 m during Irma) showed much lower values (e.g. Colombier, −2.76 m; Grande Saline, −7.64 m) (Fig. 14). On the beach scale, the site-specific characteristics, i.e. presence of rocky headlands or of a fringing reef, had a major influence on both the intensity and the spatial variability of shoreline response, for both the SL and BB indicators. For example, despite it is located on the highly-exposed northern coast, Lorient exhibited a low mean retreat NSM value (−4.46 m), due to the sheltering effect provided by the eastern rocky headland to the beach. Furthermore, the high heterogeneity of transect responses (see tables 5 and 6) on these beaches suggest that specific on-site processes also influence beach response.

Second, shoreline hardening (i.e. longitudinal structures and seaside property walls), which generally results from the partial to complete destruction of the indigenous vegetation belt for construction purposes, influenced both the intensity and spatial variability of SL positional change, and accretional vs. erosional processes (Fig. 14). Importantly, where the natural buffering area was narrow (<30 m in width) prior to the September 2017 hurricanes, the destruction of the coastal vegetation, which explains the retreat of the SL, led to the hardening of the latter, as the shoreline changed from natural before to artificial after the hurricanes. On densely urbanized beaches, this led to a marked increase in the length of the armoured shoreline. By interfering with natural processes, in particular through enhanced wave reflection, shoreline hardening also promoted sediment loss. Moreover, it limited hurricane-induced sediment inputs (e.g. sand sheets), which only occurred in localized areas (e.g. axis of beach accesses). By affecting negatively the sediment budget of beaches (i.e. causing increased sediment ablation and decreased sediment deposition) and the state of beach systems on the whole (through the total destruction of the narrow vegetation belt in front of human assets), shoreline hardening exacerbated hurricane impacts. Additionally, it weakened the vegetated beach or beach-dune system serving as a buffer in the face of hurricane waves. As a

result, coastal human assets are now much more exposed to hurricanes that they were before the September 2017 hurricanes.

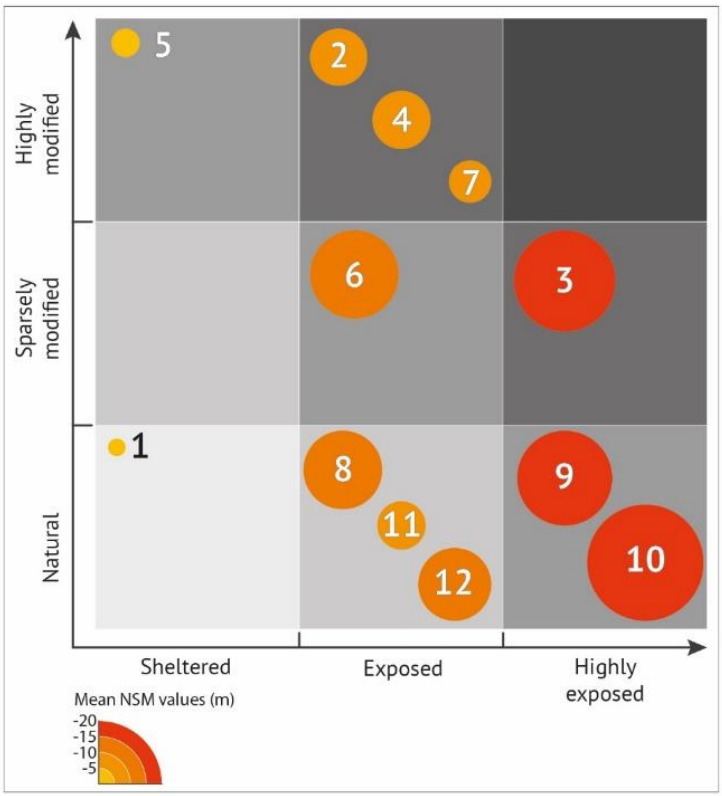

Fig. 14. Matrix of shoreline (SL) response, depending on beach exposure to hurricane waves and the disruption of natural processes by human disturbances. Here, human disturbances refer to shoreline hardening and vegetation modification. This figure suggests that the highly-exposed (i.e. eastern and northern) coasts suffered the highest SL retreat, while the sheltered (i.e. southern and western, and/or protected by a rocky headland) beaches exhibited lower SL retreat values. It also shows that shoreline positional change was greater on natural sites compared to modified sites, due to the greater resistance of the armoured shoreline to the hurricane waves.

5.2 Assessing tropical cyclones impacts on highly-modified coasts

Geomatics and satellite imagery analysis are widely used to assess changes in the position of the shoreline at different timescales (i.e. from event-related to multi-decadal) on tropical islands (among others, Webb and Kench, 2010; Ford, 2012; 2013; Yates et al., 2013; Mann and Westphal, 2014; Ford and Kench, 2014; 2015; McLean and Kench, 2015; Mann et al., 2016; Duvat et al., 2017b, c; Kench et al., 2018). While the uncertainties related to the use of geomatics in the assessment of long-term shoreline and beach change were extensively addressed by previous studies (Anders and Byrnes, 1991; Fletcher et al., 2003; Thieler and Danforth, 1994; Ford, 2012; Yates

et al., 2013), few studies dealt with the uncertainties related to the assessment of cyclone-induced shoreline and beach change (Duvat et al., 2017b). Yet, because satellite imagery only provides 2-axis data (i.e. x, y), satellite image interpretation can generate errors. First, cyclone-generated sand sheets (which constitute an accretional feature) and soil scouring (i.e. an erosional feature) can be confused when interpreting satellite images, as both are indicated by the occurrence of a sandy texture. Second, it may be challenging to distinguish remaining (i.e. still alive and able to re-grow) from uprooted (i.e. destroyed) vegetation based on image interpretation. Yet, such a distinction is key to position adequately the post-cyclone stability line. Third, because they are located in inner, i.e. often vegetated, areas, most accretional features are undetectable on satellite imagery. As a consequence, they are either under-estimated, or unconsidered in image-based studies, which therefore put more emphasis on the erosional (shown by shoreline retreat) compared to the constructional impacts of TCs. Fourth and lastly, detecting hardened shoreline may be even more challenging where the vegetation cover masks human-built structures. To overcome these four major difficulties, the conduction of field surveys –even if the latter were to occur several weeks after the cyclonic event– is urgently required. Doing so, we were able to properly take stock of erosional vs. accretional features and to increase the robustness of the data and results generated. However, the lack of pre-hurricane beach monitoring and of Digital Elevation Model, due to the remoteness of such islands, prevented us from estimating changes in beach volume. The promotion of coastal observatories in such territories would help remedy to existing limitations in beach behaviour understanding.

Additionally, based on a new methodological protocol using geomatics, this paper provides the first quantitative assessment of the influence of human disturbances on beach response to TCs. By documenting the nature of the shoreline and the distance of human-built structures to the vegetation line, and using the same DSAS transects in ArcGIS to cross-analyze shoreline- and human features-related data, we were able to discriminate natural (i.e. undisturbed) from human-driven (i.e. disturbed) modes of change, and beyond that, to quantitatively measure the role of human disturbances in increasing hurricane-induced sediment loss and shoreline hardening. Moreover, the methodology used in this paper allowed to estimate the critical distance (i.e. 30 m) at which human constructions may, in the event of an intense hurricane, have a highly-destructive impact on beach systems (i.e. cause marked sediment ablation and total vegetation destruction), which in turn exacerbates the exposure of these constructions to future hurricanes. Thus, including human disturbances in shoreline change assessment allows moving forward in attributing the spatial variability of hurricanes impacts to specific anthropogenic drivers. The protocol used is replicable and can be applied to any other coastal area.

5.3 Implications for disaster risk reduction policies and for future coastal development

Collectively, our findings have major implications for disaster risk reduction policies and future coastal development. The results obtained highlight that the more severe impacts were observed within a 30 m-wide strip from the pre-hurricane vegetation line. Furthermore, by mapping human structures, i.e. the seaward limit of buildings and of longitudinal protection structures (i.e. seawalls and ripraps), and investigating their influence on beach response to hurricane waves, we were able to emphasize that hard structures built within a 30 m-wide coastal strip from the pre-hurricane vegetation line exacerbated sediment loss and beach destabilization. Collectively, these findings advocate for the establishment of appropriate coastal development setback guidelines. In the Caribbean, most islands have setback guidelines, the setback line ranging from 15 m (in the British Virgin Islands) to 30 m (in Barbados) from the high-water mark, depending on the country considered (Cambers, 2009). On this point, our study clearly demonstrates that such setback lines are insufficient for the coastal system to absorb the energy of hurricane-generated waves and thus efficiently protect human assets from hurricane wave-induced destruction. Based on the results of this study, we recommend the establishment of a 50 m-setback for future coastal development, as this would first, allow reducing considerably the destructive impacts of hurricane waves on both beach systems (given the resistance of and sediment trapping by the indigenous vegetation >30 m from the pre-hurricane vegetation line) and coastal human assets (that would hence be effectively protected), and second, maintaining a 20 m-wide buffering area after a hurricane, which is critical not only in the case of occurrence of a new event but also to allow natural vegetation regrowth after a destructive event. Indeed, the persistence of an indigenous vegetation belt on the upper or back beach after a hurricane is key to rapid vegetation regrowth on the devastated part of the upper beach. Such setback guidelines would allow avoid the critical situation observed after the September 2017 hurricanes, in which extended urbanized shoreline sections exhibited a very high level of exposure to waves due to the total destruction of the pre-hurricane narrow buffering area by the hurricane waves. Such an increase in exposure is susceptible to cause increased damage in the event of a new hurricane. Therefore, those beaches along which the shoreline has changed from natural before the hurricanes to artificial after these events (as a result of vegetation destruction) should be considered as priority action areas for natural buffer restoration by the local authorities. All the more that the longitudinal protection structures that have resisted to the hurricane waves have generally been damaged or destabilized, which has altered their protection function. In this latter case, in the short-term, two solutions can be considered in order to reduce the future risks of impacts by hurricanes, depending on beach site characteristics. The first solution is to restore a sufficiently wide (i.e. 50 m-wide) and fully functional buffering area, that is, a complete vegetated beach or beach-dune system, depending on the setting. This would imply, first, to carry out beach or beach-dune nourishment (to compensate hurricane-

induced sediment loss) and profiling, and second, to stabilize the restored coastal system by the plantation of indigenous vegetation on the upper and back beach and front dune. This solution would have two positive effects, i.e. first, increase human assets protection from future hurricane destruction, and second, improve landscape integration of coastal constructions, which would be favourable to tourism, especially when high-end services are offered. Our findings on the positive role of the indigenous vegetation in dissipating hurricane waves and reducing their destructive impacts on back beaches and human assets, and in trapping sediment, advocate for this solution, aimed at "working with natural processes" (Cooper and McKenna, 2008). The second solution is to erect proper, i.e. well-designed and calibrated, engineering structures to fix the shoreline and prevent wave impact on human constructions. This solution would allow reducing risks on an island where most structures are handmade and generally under-calibrated to resist to category 4 and 5 hurricane waves. However, such a solution would likely have detrimental impacts on tourism, as it often contributes to beach loss while also spoiling the initially highly-attractive coastal landscape of islands. Therefore, reducing shoreline hardening not only in areas where the shoreline changed from natural to artificial, but also in areas where the shoreline was already artificial prior to the September 2017 hurricanes, through the restoration of functional buffering beach and beach-dune systems, constitutes a key area (and opportunity) for disaster risk reduction. In the long-term, other solutions could be examined, such as the relocation of the human assets that are located in highly-exposed areas.

6. Conclusion

Based on a combined approach between geomatics (i.e. shoreline change analysis using satellite imagery) and fieldwork (to take stock of accretional vs. erosional features and processes), we provide a full-spectrum analysis of the impacts of September 2017 hurricanes –Irma was the most intense hurricane ever recorded in the Lesser Antilles– on the beaches of Saint-Barthélemy Island. In line with previous studies, our results highlight the key role of low-frequency high-intensity events in driving high rates of changes on small tropical islands' sedimentary coastal systems. At all beach sites, the hurricanes caused a marked retreat of the stability line (i.e. mean NSM ranging from −2.76 m to −18.39 m, with a minimum NSM value that reached −61.82 m). However, SL retreat was lower on highly-modified beaches where longitudinal structures resisted to the hurricane waves compared to natural beaches that suffered severe vegetation destruction. Erosional features were found at all the surveyed sites, however varying considerably in intensity depending on a site's natural and anthropogenic characteristics. Beach lowering was found to be greater on densely urbanized beaches (e.g. −2.00 m at Flamands in front of longitudinal structures) than on natural beaches (e.g. −0.20 m at Petit Cul-de-Sac). In addition, fieldwork revealed that accretional features mainly formed on the back beach (i.e. sand sheets) of unbuilt sites where no human

construction obstructed sediment transport pathways, except at one site (i.e. Grand Fond), where a 1.50 m-high and 100 m-long storm ridge was found in the active beach zone. Furthermore, the coastal vegetation was largely destroyed (i.e. uprooting, trunks and branches breaking, salt-burning of leaves) along all natural shoreline sections. However, the buffering role of the remaining indigenous vegetation allowed the vertical accretion of upper beaches and of inner land areas through sediment trapping on natural beach sites.

Combining geomatics and fieldwork, we were able to attribute measured changes to specific drivers. Importantly, we found that both natural (i.e. the hurricanes' tracks and hurricane waves' direction) and anthropogenic (especially shoreline hardening and vegetation modification) drivers explain the high variability observed in the nature (i.e. erosional vs. accretional), intensity (shoreline change rates) and spatial distribution (on the island and beach scale) of September 2017 hurricanes impacts on Saint-Barthélemy beaches. Natural drivers (e.g. hurricane waves' direction, a site's geomorphic characteristics) were found to play a key role in controlling the variability of impacts on the island scale, while anthropogenic disturbances proved to control variability on the beach scale. Together, geomatics and fieldwork allowed quantifying the impacts of anthropogenic disturbances on beach response to hurricane events. Regarding the major control exerted by hurricanes on shoreline changes in small tropical islands and the high level of human asset (i.e. population, buildings, roads…) exposure to sea-related hazards and critical importance of beaches for tourism on these islands, the results obtained advocate for the restoration, wherever possible, of a functional buffering beach or beach dune systems, in order to better protect human constructions from hurricane destruction while also maintaining the quality of beaches. This in turn implies to adopt appropriate setback guidelines, i.e. to establish setback lines of approximately 50 m from the vegetation line.

Abstract

Based on an approach coupling geomatics (i.e. satellite imagery analysis) and fieldwork, this paper provides an in-depth analysis of the impacts of September 2017 hurricanes on the beaches of Saint-Barthélemy Island. First, it highlights the key role of low-frequency high-intensity events in driving high rates of changes on coastal systems. Importantly, all the studied beaches underwent shoreline retreat, detected along 47.73 to 100.00% of transects (mean shoreline movement ranging from −2.76 to −18.39 m). The stability line retreat was lower on highly-modified beaches because of the presence of longitudinal structures compared to natural beaches that mostly suffered severe vegetation destruction. Second, the methodology proposed here allowed attributing changes to specific anthropogenic drivers. Both natural (i.e. the hurricane's path and hurricane waves' direction) and anthropogenic (especially shoreline hardening and vegetation modification) drivers explain the high variability observed in the nature, intensity and spatial distribution of hurricanes' impacts on beaches. Based on the quantitative assessment of impacts, this paper advocates for the restoration of a 50 m-wide buffering area in front of human constructions, the exposure of which has considerably increased due to wave impact, which implies to establish new setback guidelines. So as to better assist decision-makers in disaster risk reduction on small islands, we therefore recommend the systematic inclusion, i.e. documentation and integration into GIS datasets, of human disturbances, as the latter highly influence shoreline and beach response. We propose a replicable methodology to address this challenge.

Keywords: Small islands, hurricanes, shoreline change, human disturbances, Lesser Antilles

Acknowledgements

V.P. and V.D. were funded by the French CNRS and by the French National Research Agency under the STORISK research project (No.ANR-15-CE03-0003). Y.K., R.C. and G.A. were funded by the ERDF/C3AF research project. All authors also got funding from the French National Research Agency under the TIREX (No. ANR-18-OURA-002-03) research project. The authors thank Benoît Simon-Bouhet for contributing to the statistical analysis. They acknowledge the reviewers for their helpful comments on this manuscript.

References

Anders FJ, Byrnes MR (1991) Accuracy of shoreline change rates as determined from maps and aerial photographs. Shore Beach 17–26

Angelucci F, Conforti P (2010) Risk management and finance along value chains of Small Island Developing States. Evidence from the Caribbean and the Pacific. Food Policy 35:565–575. doi: 10.1016/j.foodpol.2010.07.001

Aslam M, Kench PS (2017) Reef island dynamics and mechanisms of change in Huvadhoo Atoll, Republic of Maldives, Indian Ocean. Anthropocene 18:57–68. doi: 10.1016/j.ancene.2017.05.003

Baines GBK, Beveridge PK, Maragos JE (1974) Storms and island building at Funafuti Atoll, Ellice Islands. Proc 2nd Int Coral Reef Symp 2 485–496

Baines GBK, McLean RF (1976) Re-surveys of 1972 Hurricane Rampart of Funafuti Atoll, Ellice Islands. Search 7:36–37

Bayliss-Smith TP (1988) The Role of Hurricanes in the Development of Reef Islands, Ontong Java Atoll, Solomon Islands. Geogr J 154:377–391

Berg R (2018) National Hurricane Center Tropical Cyclone Report: Hurricane Jose. Natl Hurric Cent Trop Cyclone Rep 1–36. doi: AL142016

Biribo N, Woodroffe CD (2013) Historical area and shoreline change of reef islands around Tarawa Atoll, Kiribati. Sustain Sci 8:345–362. doi: 10.1007/s11625-013-0210-z

Bush DM (1991) Impact of Hurricane Hugo on the Rocky Coast of Puerto Rico. J Coast Res 49–67

Cahoon DR, Hensel P, Rybczyk J, et al (2003) Mass tree mortality leads to mangrove peat collapse at Bay Islands, Honduras after Hurricane Mitch. J Ecol 91:1093–1105. doi: 10.1046/j.1365-2745.2003.00841.x

Cambers G (2009) Caribbean beach changes and climate change adaptation. Aquat Ecosyst Heal Manag 12:168–176. doi: 10.1080/14634980902907987

Cangialosi JP, Latto AS, Berg R (2018) National Hurricane Center Tropical Cyclone Report: Huricane Irma (AL12017), 30 August-12 September 2017. Natl Huricane Cent 1–111. doi: 10.1097/TA.0000000000002006

Caron V (2011) Contrasted textural and taphonomic properties of high-energy wave deposits cemented in beachrocks (St. Bartholomew Island, French West Indies). Sediment Geol 237:189–208. doi: 10.1016/j.sedgeo.2011.03.002

Caron V (2012) Geomorphic and Sedimentologic Evidence of Extreme Wave Events Recorded by Beachrocks : A Case Study from the Island of St . Bartholomew (Lesser Antilles). 811–828. doi: 10.2112/JCOASTRES-D-10-00152.1

Cazes-Duvat V (2005) Les impacts du cyclone Kalunde sur les plages de l'Île Rodrigues (océan Indien occidental), Zeitschrift Für Geomorphologie, 49 (3): 293-308.

Cécé R, Bernard D, d'Alexis C, Dorville J-F (2014) Numerical Simulations of Island-Induced Circulations and Windward Katabatic Flow over the Guadeloupe Archipelago. Mon Weather Rev 142:850–867. doi: 10.1175/MWR-D-13-00119.1

Cécé R, Bernard D, Brioude J, Zahibo N (2016) Microscale anthropogenic pollution modelling in a small tropical island during weak trade winds: Lagrangian particle dispersion simulations using real nested LES meteorological fields. Atmospheric Environment, 139 :98-112. doi : https://doi.org/10.1016/j.atmosenv.2016.05.028.

Christman RA (1953) Geology of St. Bartholomew, St. Martin and Anguila, Lesser Antilles. Bull Geol Soc Am 64:85–96

Cooper JAG, Jackson DWT, Gore S (2013) A groundswell event on the coast of the British Virgin Islands: spatial variability in morphological impact. J Coast Res 65:696–701. doi: 10.2112/SI65-118.1

Cooper JAG, Mckenna J (2008) Working with natural processes: The challenge for coastal protection strategies. Geogr J 174:315–331. doi: 10.1111/j.1475-4959.2008.00302.x

Cooper JAG, Pile J (2014) The adaptation-resistance spectrum: A classification of contemporary adaptation approaches to climate-related coastal change. Ocean Coast Manag 94:90–98. doi: 10.1016/j.ocecoaman.2013.09.006

Degrace JN (2017) Passage de l'Ouragan Exceptionnel Irma sur les Iles Françaises des Antilles les 5 et 6 septembre 2017. Com. De Presse Meteo-France, Fort de France, 6

Duvat V (2008) Le système du risque à Saint-Martin (Petites Antilles françaises). Développement durable Territ 11:2–21. doi: 10.4000/developpementdurable.7303

Duvat V (2013) Coastal protection structures in Tarawa Atoll, Republic of Kiribati. Sustain Sci 8:363–379. doi: 10.1007/s11625-013-0205-9

Duvat VKE, Magnan AK, Etienne S, et al (2016) Assessing the impacts of and resilience to Tropical Cyclone Bejisa, Reunion Island (Indian Ocean). Nat Hazards 1–40. doi: 10.1007/s11069-016-2338-5

Duvat VKE, Magnan AK, Wise RM, et al (2017a) Trajectories of exposure and vulnerability of small islands to climate change. Wiley Interdiscip Rev Clim Chang 8:. doi: 10.1002/wcc.478

Duvat VKE, Volto N, Salmon C (2017b) Impacts of category 5 tropical cyclone Fantala (April 2016) on Farquhar Atoll, Seychelles Islands, Indian Ocean. Geomorphology 298:41–62. doi: 10.1016/j.geomorph.2017.09.022

Duvat VKE, Salvat B, Salmon C (2017c) Drivers of shoreline change in atoll reef islands of the Tuamotu Archipelago, French Polynesia. Glob Planet Change 158:134–154. doi: 10.1016/j.gloplacha.2017.09.016

Duvat VKE, Pillet V (2017) Shoreline changes in reef islands of the Central Pacific: Takapoto Atoll, Northern Tuamotu, French Polynesia. Geomorphology 282:96–118. doi: 10.1016/j.geomorph.2017.01.002

Duvat V, Pillet V, Volto N, et al (2019) High human influence on beach response to tropical cyclones in small islands: Saint-Martin Island, Lesser Antilles. Geomorphology 325:70–91. doi: 10.1016/j.geomorph.2018.09.029

Emanuel K, Rotunno R (2011) Self-stratification of tropical cyclone outflow, Part I: Implications for storm structure. J. Atmos. Sci., 68, 2236–2249

Etienne S (2012) Marine inundation hazards in French Polynesia: geomorphic impacts of Tropical Cyclone Oli in February 2010. Geol Soc London, Spec Publ 361:21–39. doi: 10.1144/SP361.4

Fielding R (2017) Landscapes and Landforms of the Lesser Antilles. 45–59. doi: 10.1007/978-3-319-55787-8

Fletcher C, Richmond B, Rooney J, et al (2003) Mapping Shoreline Change Using Digital Orthophotogrammetry on Maui, Hawaii. J Coast Res SPEC ISS 38:106–124

Fletcher CH, Mullane RA, Richmond BM, et al (1997) Beach Loss Along Armored Shorelines on Oahu, Hawaiian Islands. J Coast Res 13:209–215

Ford M (2012) Shoreline Changes on an Urban Atoll in the Central Pacific Ocean : Majuro Atoll , Marshall Islands. 11–22. doi: 10.2112/JCOASTRES-D-11-00008.1

Ford M (2013) Shoreline changes interpreted from multi-temporal aerial photographs and high resolution satellite images: Wotje Atoll, Marshall Islands. Remote Sens Environ 135:130–140. doi: 10.1016/j.rse.2013.03.027

Ford MR, Kench PS (2014) Formation and adjustment of typhoon-impacted reef islands interpreted from remote imagery: Nadikdik Atoll, Marshall Islands. Geomorphology 214:216–222. doi: 10.1016/j.geomorph.2014.02.006

Ford MR, Kench PS (2015) Multi-decadal shoreline changes in response to sea level rise in the Marshall Islands. Anthropocene 11:14–24. doi: 10.1016/j.ancene.2015.11.002

Ford MR, Kench PS (2016) Spatiotemporal variability of typhoon impacts and relaxation intervals on Jaluit Atoll, Marshall Islands. 44:159–162. doi: 10.1130/G37402.1

Giuliani G, Peduzzi P (2011) The PREVIEW global risk data platform: A geoportal to serve and share global data on risk to natural hazards. Nat Hazards Earth Syst Sci 11:53–66. doi: 10.5194/nhess-11-53-2011

Hay J, Mimura N (2010) The changing nature of extreme weather and climate events: risks to sustainable development. Geomatics, Nat Hazards Risk 1:3–18. doi: 10.1080/19475701003643433

Holland G (1980) An Analytic Model of the Wind and Pressure Profiles in Hurricanes. Mon. Weather Rev., 108, 1212–1218.

Kench PS, Ford MR, Owen SD (2018) Patterns of island change and persistence offer alternate adaptation pathways for atoll nations. Nat Commun. doi: 10.1038/s41467-018-02954-1

Kench PS, Thompson D, Ford MR, et al (2015) Coral islands defy sea-level rise over the past century: Records from a central Pacific atoll. Geology 43:515–518. doi: 10.1130/G36555.1

Krien Y, Arnaud G, Cécé R, Ruf C, Belmadani A, Khan J, Bernard D, Islam A.K.M.S., Durand F, Testut L, Palany P, Zahibo N (2018) Can We Improve Parametric Cyclonic Wind Fields Using Recent Satellite Remote Sensing Data? Remote Sens., 10, 1963; doi:10.3390/rs10121963

Mallela J, Crabbe MJC (2009) Hurricanes and coral bleaching linked to changes in coral recruitment in Tobago. Mar Environ Res 68:158–162. doi: 10.1016/j.marenvres.2009.06.001

Mann T, Bayliss-Smith T, Westphal H (2016) A Geomorphic Interpretation of Shoreline Change Rates on Reef Islands. J Coast Res 32:500–507. doi: 10.2112/JCOASTRES-D-15-00093.1

Mann T, Westphal H (2014) Assessing long-term changes in the beach width of reef Islands based on temporally fragmented remote sensing data. Remote Sens 6:6961–6987. doi: 10.3390/rs6086961

Maragos JE, Baines GBK, Beveridge PJ (1973) Tropical Cyclone Bebe Creates a New Land Formation on Funafuti Atoll. Science (80-) 181:1161–1164. doi: 10.1126/science.181.4105.1161

McLean R, Kench P (2015) Destruction or persistence of coral atoll islands in the face of 20th and 21st century sea-level rise? Wiley Interdiscip Rev Clim Chang n/a-n/a. doi: 10.1002/wcc.350

Morton RA, Richmond BM, Jaffe BE, Gelfenbaum G (2008) Coarse-Clast Ridge Complexes of the Caribbean: A Preliminary Basis for Distinguishing Tsunami and Storm-Wave Origins. J Sediment Res 78:624–637. doi: 10.2110/jsr.2008.068

Nurse LA, McLean RF, Agard J, et al (2014) Small islands. In: Barros VR, Field CB, Dokken DJ, et al. (eds) Climate Change 2014: Impacts, Adaptation, and Vulnerability. Part B: Regional Aspects. Contribution of Working Group II to the Fifth Assessment Report of the Intergovernmental Panel of Climate Change. Cambridge University Press, Cambridge, United Kingdom and New York, NY, USA, pp 1613–1654

Pelling M, Uitto J (2001) Small island developing states: natural disaster vulnerability and global change. Glob Environ Chang Part B Environ Hazards 3:49–62. doi: 10.1016/S1464-2867(01)00018-3

Rankey EC (2011) Nature and stability of atoll island shorelines: Gilbert Island chain, Kiribati, equatorial Pacific. Sedimentology 58:1831–1859. doi: 10.1111/j.1365-3091.2011.01241.x

Rey T, Dé L Le, Leone F, David G (2017) Leçons tirées du cyclone Pam au Vanuatu (Mélanésie) : aléas côtiers, crues éclairs et dommages. Géomorphologie Reli Process Environ 23:. doi: 10.4000/geomorphologie.11842

Rivera-Monroy V., Twilley R., Weil E (2004) A conceptual framework to develop long-term ecological research and management objectives in the wider Caribbean region. Bioscience 54:843–856. doi: 10.1641/0006-3568(2004)054[0843:ACFTDL]2.0.CO;2

Romine BM, Fletcher CH (2012) Armoring on Eroding Coasts Leads to Beach Narrowing and Loss on Oahu, Hawaii. In: Cooper JAG, Pilkey OH (eds) Pitfalls of Shoreline Stabilization: Selected Case Studies. Springer Netherlands, Dordrecht, pp 141–164

Salmon C, Duvat VKE, Laurent V (2019) Human- and climate-driven shoreline changes on a remote mountainous tropical Pacific Island: Tubuai, French Polynesia. Anthropocene 25:100191. doi: 10.1016/J.ANCENE.2019.100191

Scheffers A, Scheffers S (2006) Documentation of the Impact of Hurricane Ivan on the Coastline of Bonaire (Netherlands Antilles). J Coast Res 1437–1450. doi: 10.2112/05-0535.1

Schlacher TA, Schoeman DS, Lastra M, et al (2006) Neglected ecosystems bear the brunt of change. Ethol Ecol Evol 18:349–351. doi: 10.1080/08927014.2006.9522701

Scoffin TP (1993) The geological effects of hurricanes on coral reefs and the interpretation of storm deposits. Coral Reefs 12:203–221. doi: 10.1007/BF00334480

Scopélitis J, Andréfouët S, Phinn S, et al (2009) Changes of coral communities over 35 years: Integrating in situ and remote-sensing data on Saint-Leu Reef (la Réunion, Indian Ocean). Estuar Coast Shelf Sci 84:342–352. doi: 10.1016/j.ecss.2009.04.030

Skamarock WC, Klemp JB (2008) A time-split nonhydrostatic atmospheric model for weather research and forecasting applications. J Comput Phys 227:3465–3485. doi: 10.1016/j.jcp.2007.01.037

Stoddart DR (1963) Effects of hurricane Hattie on the British Honduras reefs and cays, October 30-31, 1961, Atoll Research Bulletin 95: 1-142.

Stoddart DR (1965) The shape of atolls. Mar Geol 3:369–383. doi: 10.1016/0025-3227(65)90025-3

Strobl E (2012) The economic growth impact of natural disasters in developing countries: Evidence from hurricane strikes in the Central American and Caribbean regions. J Dev Econ 97:130–141. doi: 10.1016/j.jdeveco.2010.12.002

Thieler ER, Danforth WW (1994) Historical Shoreline Mapping (I): Improving Techniques and Reducing Positioning Errors. J Coast Res 10:549–563

Thieler ER, Himmelstoss EA, Zichichi JL, Ergul A (2017) The Digital Shoreline Analysis System (DSAS) Version 4.0 - An ArcGIS extension for calculating shoreline change (ver. 4.4, July 2017) : U.S. Geological Survey Open-File Report 2008-1278. Reston

Webb AP, Kench PS (2010) The dynamic response of reef islands to sea-level rise: Evidence from multi-decadal analysis of island change in the Central Pacific. Glob Planet Change 72:234–246. doi: 10.1016/j.gloplacha.2010.05.003

Yates ML, Le Cozannet G, Garcin M, et al (2013) Multidecadal Atoll Shoreline Change on Manihi and Manuae, French Polynesia. J Coast Res 289:870–882. doi: 10.2112/JCOASTRES-D-12-00129.1

Zhang YJ, Ye F, Stanev E V., Grashorn S (2016) Seamless cross-scale modeling with SCHISM. Ocean Model 102:64–81. doi: 10.1016/j.ocemod.2016.05.002

Supplementary Material

Beach number and name	Pre-hurricane					Post-hurricane				
	Total length (m)	Natural		Artificial		Total length (m)	Natural		Artificial	
		Length (m)	%	Length (m)	%		Length (m)	%	Length	%
1. Colombier	338.73	338.73	100.00	0	0.00	331.94	331.94	100	0	0.00
2. Flamands	767.08	715.54	93.28	51.54	6.72	916.76	337.39	36.8	579.37	63.2
3. Cayes	670.77	606.28	90.39	64.49	9.61	1035.63	676.23	65.3	359.4	34.7
4. Saint-Jean	1135.6	812.98	71.59	322.62	28.41	1246.85	667.17	53.51	579.68	46.49
5. Lorient	1046.35	752.69	71.93	293.66	28.07	1222.33	492.71	40.31	729.62	59.69
6. Marigot	217.6	217.6	100.00	0	0.00	260.18	248.56	95.53	11.63	4.47
7. Grand Cul-de-Sac	760.57	613.33	80.64	147.24	19.36	1241.21	784.35	63.19	456.86	36.81
8. Petit Cul-de-Sac	467.15	467.15	100.00	0	0.00	822.98	737.3	89.59	85.68	10.41
9. Toiny	506.05	506.05	100.00	0	0.00	657.26	657.26	100	0	0.00
10. Grand Fond	635.01	635.01	100.00	0	0.00	722.23	619.36	85.76	102.86	14.24
11. Grande Saline	1263.53	1263.53	100.00	0	0.00	1161.57	1161.57	100	0	0.00
12. Gouverneur	424.45	424.45	100.00	0	0.00	470.97	470.97	100	0	0.00

SM 1. Length of natural and artificial shoreline before and after September 2017 hurricanes.